

Article

Multidecadal Phase Changes in the Thermodynamic State of the System: Ocean–Atmosphere–Continent

Vladimir Byshev ¹, Anatoly Gusev ^{1,2,3,*} and Alexandra Sidorova ¹

¹ Shirshov Institute of Oceanology, Russian Academy of Sciences, Moscow 117997, Russia; byshev.v@mail.ru (V.B.); sandra.sn@mail.ru (A.S.)

² Marchuk Institute of Numerical Mathematics, Russian Academy of Sciences, Moscow 119333, Russia

³ Zubov State Oceanographic Institute, Roshydromet, Moscow 119034, Russia

* Correspondence: anatoly.v.gusev@gmail.com

Abstract: The present-day climate (the recent 100–150 years) obviously constitutes the structure of a global intra-system rhythmic process with an individual rhythm of about 60 years. In turn, each of the rhythms is presented by the two climate phases of about 25–35 years characterized by qualitative differences: one phase is relatively continental, while the other is humid. Globality and quasi-synchronism of environmental changes are accompanied by planetary structures: the Global Atmospheric Oscillation (GAO) in the atmosphere and the Multidecadal Oscillation of the Heat content in the Ocean (MOHO) discovered relatively recently. Unexpected and rapid qualitative phase changes in the climate, which first focused attention in the mid-1970s of the last century, were titled “climate shifts”. The revealed features of the present-day climate are of exceptional scientific and practical interest and deserve the development of methods for predicting the timing of the forthcoming climate shift. Arising unexpectedly and accompanied by rapid significant changes, these shifts identified the problem of understanding the nature and establishing the processes and mechanisms causing them. First of all, of interest are phase changes in the thermodynamic state of the climate system components: the ocean, atmosphere, and continents. As a result of the World Ocean (WO) thermohydrodynamics numerical modelling, it is shown that MOHO is localized in the layer of the main thermocline, where the most important elements of the WO circulation are located. The performed study based on observational data allows us to conclude that, during the phase of the WO thermal discharge (1975–1999), the two key systems of currents, the Kuroshio and the Gulf Stream, were under similar thermodynamic conditions.

Keywords: world ocean; heat content; active upper layer; variability; multidecadal oscillation; numerical modelling; present-day climate



Citation: Byshev, V.; Gusev, A.; Sidorova, A. Multidecadal Phase Changes in the Thermodynamic State of the System: Ocean–Atmosphere–Continent. *J. Mar. Sci. Eng.* **2024**, *12*, 758. <https://doi.org/10.3390/jmse12050758>

Academic Editor: Angelo Rubino

Received: 21 March 2024

Revised: 24 April 2024

Accepted: 28 April 2024

Published: 30 April 2024



Copyright: © 2024 by the authors. Licensee MDPI, Basel, Switzerland. This article is an open access article distributed under the terms and conditions of the Creative Commons Attribution (CC BY) license (<https://creativecommons.org/licenses/by/4.0/>).

1. Introduction

The present-day climate, according to current observations for the past 100–150 years, is determined by a number of characteristic features. The most significant of them are climate shifts [1–3] constituting unexpected and rapid transitions from the phase of the observed (for 25–35 years) relatively humid global climate into the phase of its essentially continental state, and then (after 25–35 years) its subsequent transition to a humid phase, etc. The search for the source of multidecadal phase changes in the global climate [4] made it possible to consider this process as an intrasystem—one supported by oscillations in the World Ocean (WO) heat content localized in the layer of the main thermocline. Thus, a feature of the present climate dynamics is episodic rapid (for 2–3 years) phase transitions of the global climate from one qualitative state to another. The globality and quasi-synchronicity of environmental changes are caused by planetary oscillations detected in both the ocean (MOHO) [5] and atmosphere (GAO) [6]. The processes and mechanisms responsible for the high intensity of climate change have been identified. Those in the atmosphere, for example,

are meridional northern and southern transports of air masses, cloudiness, precipitation, etc. In the ocean, the phenomena and processes that deserve attention are deep density convection, which ensures heat exchange of the ocean's active upper layer (AUL) with the atmosphere, transfrontal mass and heat exchange, which carries out horizontal mixing within the ocean AUL with polar and central oceanic waters, a specified variability in the water circulation regime of the main current systems of the WO, etc. The main mechanism of transfrontal exchange is the process of baroclinic instability of large-scale currents, which ensures the transition of available potential energy into the kinetic energy of mesoscale eddies [7,8]. The most significant areas of the WO forming the Earth's climate and reflecting its current changes include the systems of Western Boundary Currents (WBC), which are primarily the Kuroshio in the Pacific Ocean (PO) and the Gulf Stream in the Atlantic Ocean (AO) [9]. Each of them is characterized by extreme processes of interaction between the ocean and atmosphere [10,11]. Both current systems are associated with the frontal sections of waters of subarctic and central oceanic structures, the baroclinicity of which is most pronounced, and their instability obviously has multidecadal phase variability. Studying the evolution of the thermodynamic state of the water structure in these current systems should help deepen our knowledge of the present climate and the features of its dynamics.

The present work is dedicated to the discussion of the contemporary problem of the present-day climate: its important characteristic features and their nature. The main focus of climatologists is on global anthropogenic climate warming. The role of the influence of natural factors (participation and reflection of the WO thermodynamic state) has been overshadowed and is not a priority. In recent decades, investigations of the climate and its variability have been widely performed, using numerical modelling and computational experiments. The most well-known of such international projects are CORE (Coordinated Ocean-ice Reference Experiment) [12–16] and OMIP (Ocean Model Intercomparison Project) [17,18], which are organized in the scope of the prescribed data for the computation of atmospheric forcing, and a series of the projects CMIP (Coupled Model Intercomparison Project), the results of which were published in the reports of IPCC (Intergovernmental Panel on Climate Change) [19–21]. At the same time, in the 1970s–1980s, a number of the greatest hydrophysical experiments were carried out in the WO: "Polygon-70", "Mode-73", "Polimode (1977–78)", "Mesopolygon-85", "Megapolygon-87", "Atlantex-90", etc. The purpose of these experiments was to study the ocean eddy dynamics, and it was not assumed that their instrumental observations would be in demand in the current efforts to understand the dynamics of the contemporary climate. Of interest are the results of complex observations in the scope of programs of large-scale hydrophysical experiments carried out in these informative areas: "Megapolygon-87" [22] for the Kuroshio system and "Atlantex-90" [23] for the Gulf Stream system.

This paper proposes to come back to a critical analysis of instrumental observations of some of these experiments to study the phase climate signal in the WO (its thermodynamic state in such informative areas as the Kuroshio and Gulf Stream current systems). The goal that motivated the research undertaken is to increase our knowledge and deepen our understanding of the events and processes currently occurring in the climate system, in particular, the participation and establishment of the role of the WO.

2. Materials and Methods

In the scope of the work, the authors took advantage of the following materials:

- The results of numerical modelling of the WO thermodynamic state variability for the period 1948–2007 [24] using the OGCM (ocean general circulation model) and INMOM (Institute of Numerical Mathematics Ocean Model) [25,26];
- The results of diagnostic predictions of climate changes in the thermohaline structure of the PO northwestern region as one of the WO key areas, including the Kuroshio system [27];
- The materials from instrumental observations carried out in large-scale hydrophysical experiments "Megapolygon-87" (Pacific Ocean, 1987) [22] and "Atlantex-90" (Atlantic, 1990) [23]. One of the authors (Byshev, V.I.) directly participated as deputy head of the

expedition on the research vessel (RV) “Akademik Kurchatov” (“Megapolygon-87”) and on the RV “Vityaz” (“Atlantex-90”). Some of the observational results in these experiments, for example, the negative (!) heat balance at the ocean surface in the test site area in the warm half of the year (June–September), turned out unexpected and not understood. Currently, after establishing the temporal phase variability of the contemporary climate [28], the previously obtained results became obvious: the experiment was carried out for the phase (1975–1999) of the WO thermal discharge [5]. Establishing signs of the MOHO [5] in the main thermocline layer [4] made it possible to use the features of the WO dynamics as a new approach. Since the main thermocline layer is characterized by the main current systems of the WO, a joint consideration of the two most important of them—the Kuroshio and the Gulf Stream—is of natural interest. Of particular interest were direct instrumental observations obtained during the two large hydrophysical experiments: “Megapolygon” (Kuroshio system, 1987) and “Atlantex-90” (Gulf Stream system, 1990). Both current systems were, as noted below, in the climatic regime of WO thermal discharge.

3. Results

The results of the WO thermodynamic state variability numerical modelling for the period 1948–2007 [24] using the OGCM (ocean general circulation model) INMOM (Institute of Numerical Mathematics Ocean Model) [25,26] were used to analyze the features of the spatio-temporal thermal structure of the ocean AUL (0–800 m) areas of large-scale hydrophysical experiments “Megapolygon-87” (Figure 1) and “Atlantex-90” (Figure 2).

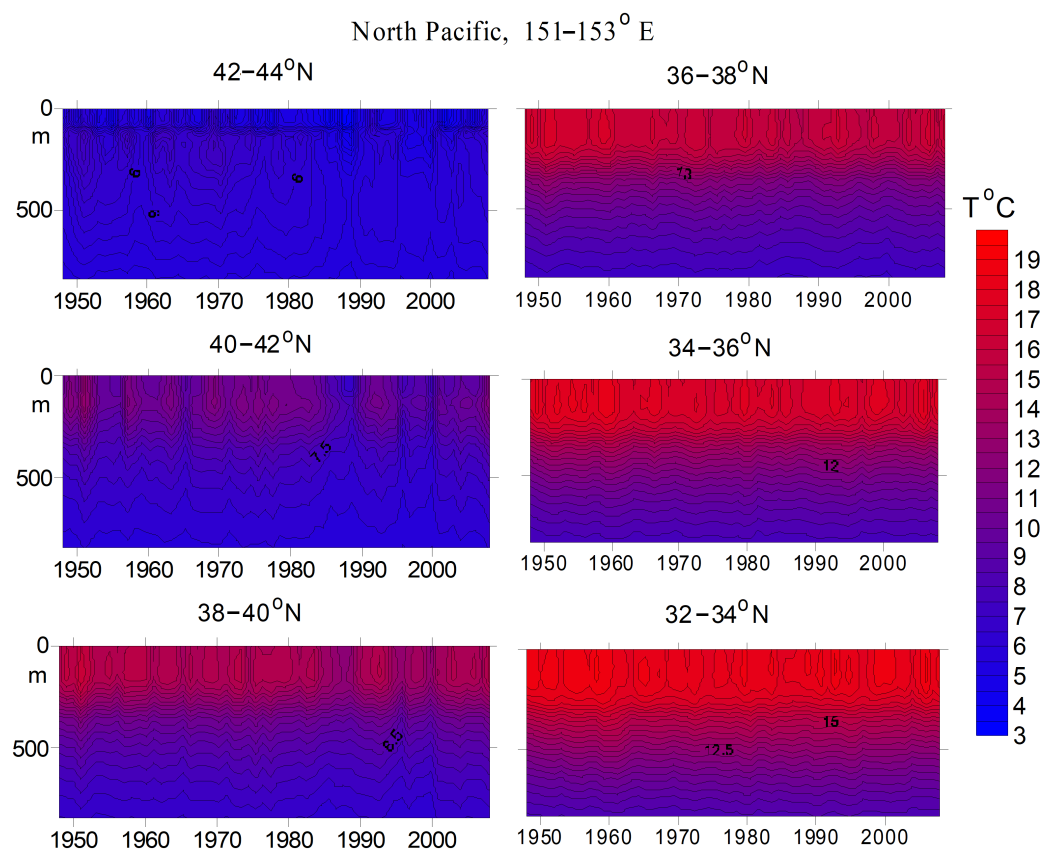


Figure 1. Evolution of the thermal structure of the AUL (0–800 m) in the PO in the area of the experiment Megapolygon in the cold part of the year (November–March) according to modelling results [24].

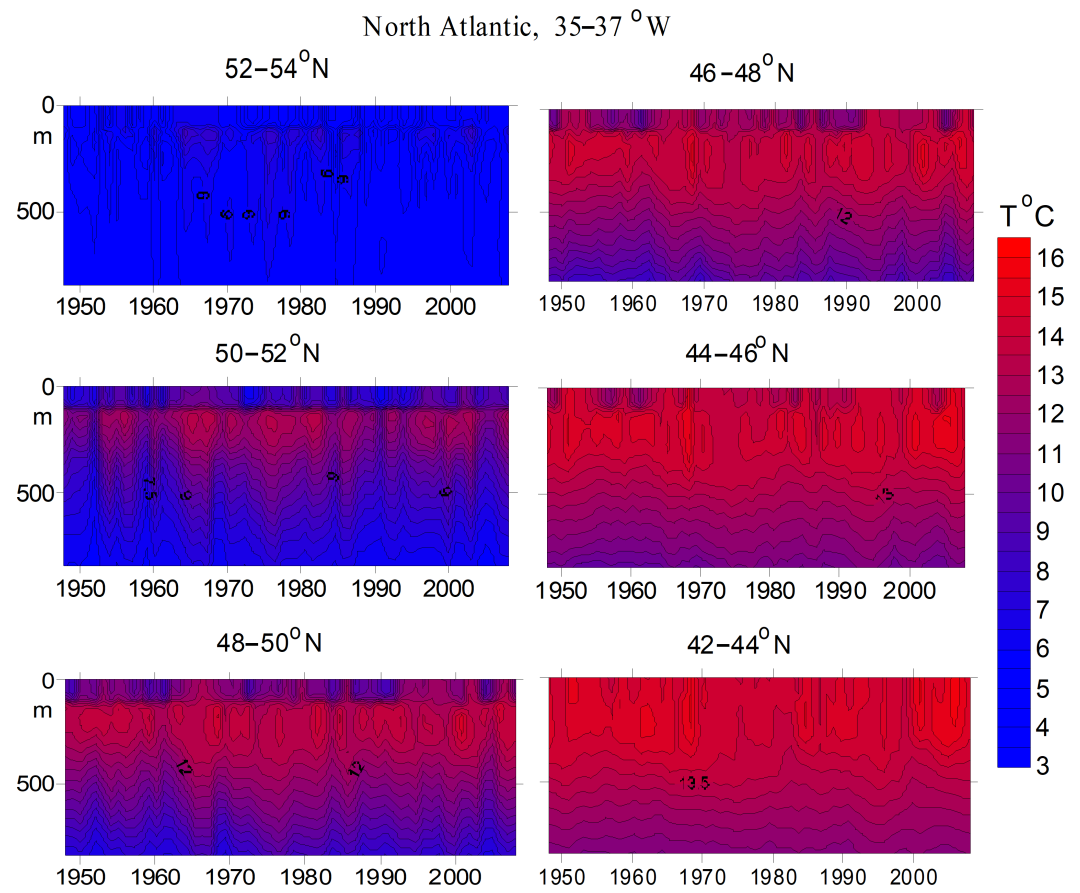


Figure 2. Evolution of the thermal structure of the AUL (0–800 m) in the North Atlantic (NA) in the area of the experiment Atlantex-90 in the cold part of the year (November–March) according to modelling results [24].

The spatiotemporal patterns of the AUL temperature in the two key WO regions (Figures 1 and 2) allow us to note the characteristic features of the water structure in the two systems of western boundary currents. In each of the regions under consideration, frontal zones are observed, which form horizontal boundaries of propagation and interaction of subarctic and central oceanic water masses, thereby determining their regional climatic significance. Of particular interest is the time interval 1975–1999, limited by the two climate shifts (mid-1970s and the eve of the 21st century) and characterized by the WO thermal discharge [4,29]. Noteworthy are specific differences in the cellular structure of quasi-homogeneous waters in the near-surface 200 m ocean layer during the indicated period and beyond it. Such a structure may reflect ongoing phase changes in both the convective regime and eddy activity.

For a number of the AUL temperature evolution features typical for the PO northwestern part (Figure 1) in the cold season (November–March), the following can be noted.

1. In the near-surface ocean layer, a quasi-homogeneous layer is well defined from 50 to 100 m in the north to 200 m in the south. A seasonal thermocline is formed at its lower boundary.
2. Deeper than the seasonal thermocline, in a layer of 200–600 m, there is a main thermocline, which, when displaced from the south (frame 32–34° N) to the north (frame 42–44° N), rises to the surface while forming a frontal interface between the subarctic and central water structures.
3. The presence and location of the frontal section are determined by significant meridional changes in the water temperature of the upper 200 m layer, which is observed

by moving from frame 42–44° N to frame 40–42° N and from the latter to the next one (38–40° N).

4. Temporal changes in the temperature field make it possible to draw attention to the disturbances on interannual (in the upper quasi-homogeneous layer) and multidecadal (in the main thermocline layer) scales.

The features of the AUL thermal structure evolution (0–800 m) in the NA (area of the Atlantex-90 experiment, Figure 2) are largely similar to those noted in the first case.

1. In the near-surface 100 m layer, there is a quasi-homogeneous layer with a seasonal thermocline at its lower boundary.
2. In the 100–800 m layer, there is a main thermocline, which rises to the ocean surface with increasing latitude (from 42° N to 50° N), forming an interface between the subarctic and central water structures. It manifests itself most expressively in the near-surface layer: in frames 48–50° N and 50–52° N (Figure 2).
3. In the area under consideration, the warm subsurface (100–300 m) layer is well expressed.
4. Temporal variability of the AUL thermal structure experiences interannual and multi-decadal perturbations.

3.1. The Experiment “Megapolygon-87”

The hydrophysical experiment “Megapolygon-87” (subarctic frontal zone of the northwestern PO, July–October 1987) was carried out in the area 37–43° N, 150–160° E with participation of the 11 RVs [30]. The frontal zone investigation was conducted using long-term measurements with a network of 177 autonomous buoy stations and six multi-vessel hydrological surveys of the area with a spatial resolution of 20 miles. Complex observations included measurements of temperature, electrical conductivity, pressure, pulsations of density and current velocity, measurements of meteorological elements, etc. Consider a number of results reflecting the thermodynamic state of the “Megapolygon-87” experiment area during the phase of WO thermal discharge (1975–1999).

An insight into the spatial temperature structure at the “Megapolygon-87” can be obtained from the materials of the hydrological survey (Figure 3) carried out during the period of 1–20 August 1987 by the RV “Akademik Kurchatov” and the RV “Vityaz”. The features of this structure are as follows.

1. The presence of subarctic waters (isotherm 2 °C) located in the northwestern sector of the test site. These waters enter here with the Kuril (Subarctic) Current propagating from west to east, forming a cyclonic vorticity.
2. The presence of relatively warm transformed waters of the main meander of the northern Kuroshio jet, the lower boundary of which (isotherm 5 °C) penetrates to a depth of 400–600 m. These waters constitute the main water mass of the upper 500 m layer between the 1st (151°24' E) and 4th (154°00' E) meridional sections, and its central part is located between the 2nd (152°50' E) and 3rd (153°44' E) sections. The dynamics of these waters have an anticyclonic vorticity: their northern boundary from the first to the second section shifts to the north, and then, from the third to the fourth sections, it shifts to the south.
3. The result of the interaction between the cold Kuril (Subarctic) Current and the transformed waters of the northern Kuroshio jet is a hydrological front that has a two-level structure, one of which lies within the upper 200 m layer and is formed by the southern border of the Kuril (Subarctic) Current, while the second one, deepening to 300–400 m, is formed by the northern boundary of the northern Kuroshio jet transformed waters.
4. Meridional sections 4 (154°00' E) and 5 (155°00' E) cross a cold cyclonic formation that moves eastward and transports a subarctic water structure.
5. In the southern part of the test site (between 38 and 39° N), waters are found whose surface temperature is 24–25 °C and higher. Their appearance is obviously due to the meandering of the main Kuroshio jet.

6. The upper quasi-homogeneous layer, below which the seasonal thermocline is located, is quite thin and ranges between 10 and 15 m in the north to 30 m or more in the south.
7. The main thermocline lies in a layer of 150–400 m between 35 and 40° N and, in the northward direction, it rises to the surface of 41–42° N (sections 151°24' E, 152°50' E, 153°44' E) and merges with the seasonal thermocline.

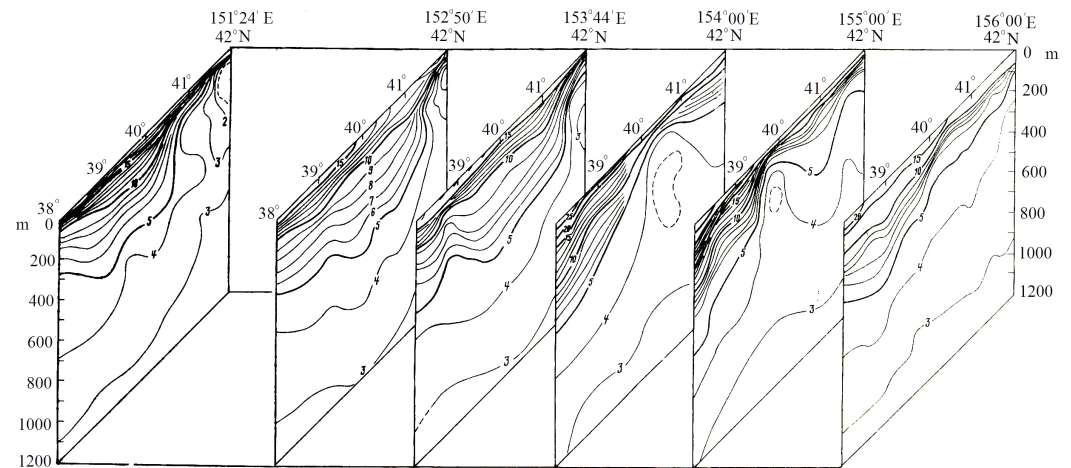


Figure 3. Three-dimensional structure of the temperature field (in °C) at the Megapolygon by the measurements made by the RV “Akademik Kurchatov” and the RV “Vityaz” in the period 1–20 August 1987 by the hydrological data survey 2. Adaptation of Figure 1 from [31].

Based on the same survey data, a map (Figure 4) of temperature distribution on a 100 m horizon was constructed. The main features of the temperature structure presented in Figure 3 also occur in this case. In particular, the two frontal sections are clearly distinguished: the northern one (isotherms 2–7 °C), which is the southern boundary of the Kuril (Subarctic) Current, and the second one (isotherms 8–10 °C), which is the northern boundary of the northern Kuroshio jet transformed waters. At a horizon of 100 m, a cold cyclonic formation is clearly manifested with the centre coordinates 40°40' N, 154°30' E, which stands out on the meridional sections (Figure 3) along 154°37' E and 155°00' E. Warm waters (isotherms 12–17 °C) apparently caused by a northward shift of the main Kuroshio jet are observed on the southern periphery of the test site. The temperature map on a 100 m horizon allows us to observe some more features of the thermal structure, such as, a warm formation with the centre coordinates 41°50' N, 154°30' E, and a cold formation with the centre coordinates 38°30' N, 153°15' E.

A map of sea surface temperature (SST) constructed by continuous measurements of the RV “Akademik Kurchatov” and RV “Vityaz” using ship-based remote thermometers (SRT) is presented in Figure 5. Continuous temperature measurements make it possible to determine the position of the frontal sections by estimating the extreme values of horizontal temperature gradients. In the northwest of the test site, the lowest water temperature recorded was 13.1–17.0 °C, which was due to the spread of subarctic waters from the north and the passage of the Kuril (Subarctic) Current jet. In the west of the region and in its central part, a fairly high SST observed was 21.0–24.4 °C. This is due to the penetration of transformed waters of the Kuroshio northern branch to this location. In the south of the region, the highest water SSTs recorded were 22.0–26.1 °C, which is associated with a shift of the main Kuroshio jet northward. The presence of warm and cold formations indicates active eddy formation in the area under study and characterizes the process of large-scale mixing in the subarctic frontal zone. The horizontal size of the largest warm and cold formations is about 100 km; small formations are 20–30 km.

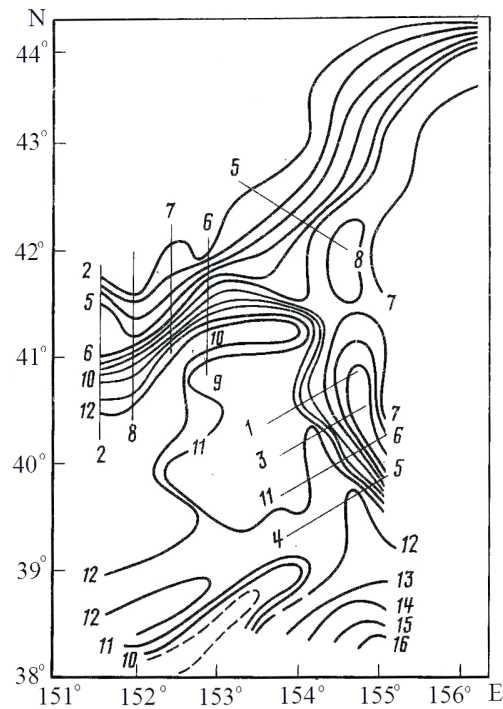


Figure 4. Distribution of water temperature (°C) on a 100 m horizon for 1–20 August 1987 from the data of the 2nd hydrological survey. Straight lines are the directions along which horizontal temperature gradients were calculated. Adaptation of Figure 2 from [31].

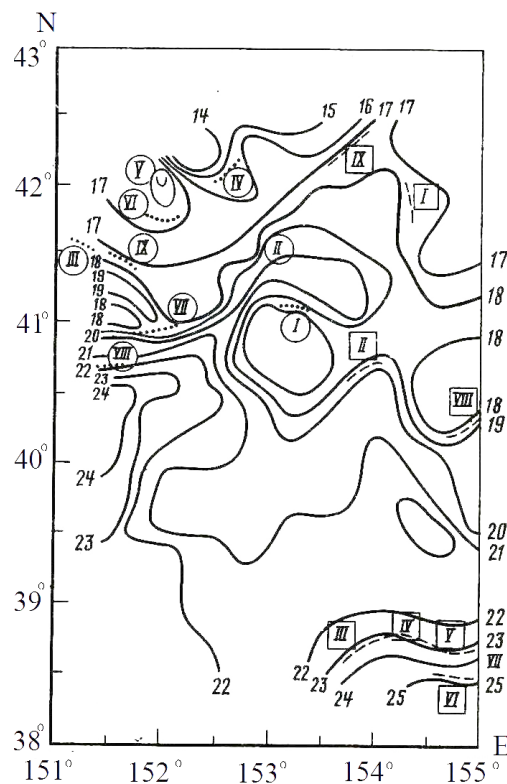


Figure 5. Distribution of SST (°C) by continuous measurements with ship-based remote thermometers in August 1987. Roman numerals mark positions of frontal sections, dash lines mark measurements by the RV "Vityaz", and dotted lines mark measurements by the RV "Akademik Kurchatov". Adaptation of Figure 3 from [31].

Fronts on the ocean surface experience continuous disturbances, the most important of which are related to their evolution and movements in space. In August 1987, the 20 °C isotherm tracks the southern boundary of the subarctic front. An idea regarding the temporal variability of the subarctic front southern branch is given in Figure 6, which shows the dynamics of the 20 °C isotherm. To construct Figure 6, 3-day synoptic SST maps transmitted from the Japanese Fisheries Service Information Center were used. An analysis of Figure 6 allows us to note a number of dynamic features for the isotherm 20 °C:

1. The temporal variability of 20 °C isotherm is significant even over 3 days.
2. There are areas on the frontal line where its transverse disturbances range from one to several degrees of latitude.
3. Nodal points are identified on the frontal line at which the lateral variability is insignificant (less than 20 min of latitude).

Such a behaviour of the frontal line has the analogue of a standing wave with distances between nodal points of about 300 km.

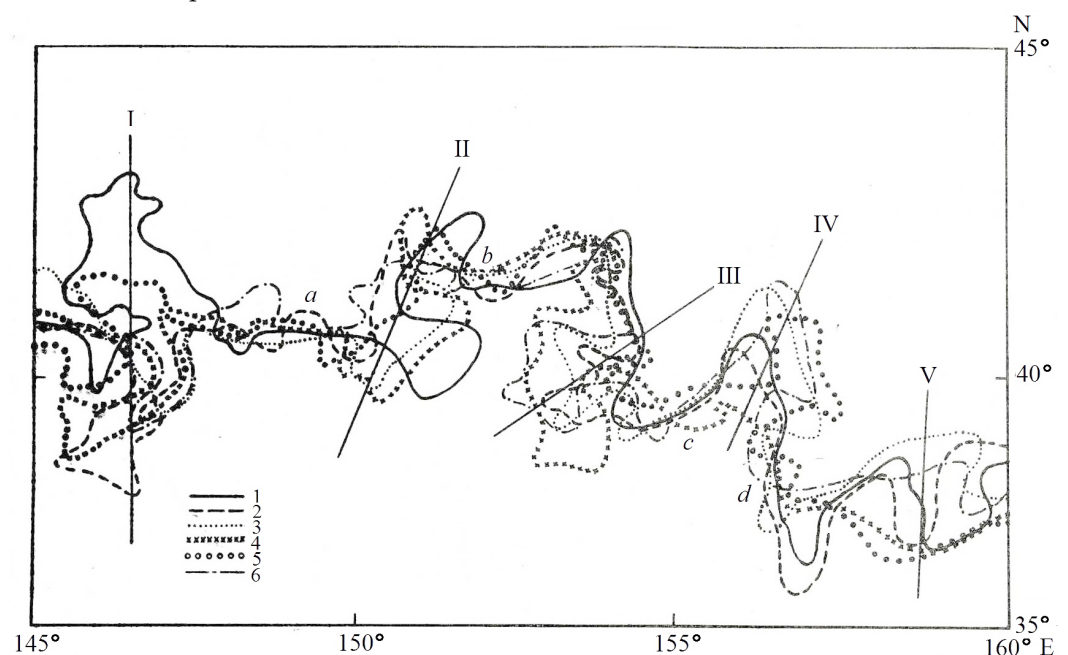


Figure 6. Position in space and time of the isotherm 20 °C in 1987. Line 1 marks 18–21 August; Line 2 marks 21–24 August; Line 3 marks 25–28 August; Line 4 marks 28–31 August; Line 5 marks 1–4 September; Line 6 marks 4–7 September; I–V are the sections. Adaptation of Figure 5 from [31].

SST temporal variability is driven by ocean–atmosphere interactions and ocean dynamic processes, some of which have time scales comparable to or shorter than the duration of the hydrological survey. We illustrate one of the variability fragments by comparing the meridional section along 155°00' E (Figure 7) made on 9 August 1987, and the same section shown in Figure 3 completed on 19 August 1987. A comparison of the two successive meridional sections indicates a similarity in the vertical structure in both cases manifested in the presence of a cold cyclonic formation in the central part of the section. However, the difference between the two structures is noteworthy, which consists in the presence of a wave-like disturbance between 38°00' N and 39°30' N in the layer from the surface to 1000 m on 9 August 1987 (see Figure 7) and in its absence on 19 August 1987 (see Figure 3). A trace of such a disturbance is apparently observed in Figure 4 (coordinates 38°30' N, 153°15' E, which shows the temperature distribution over the 100 m level).

Returning to the comparison of Figures 3 and 7, we can note a different phase of the cold cyclonic formation movement, so if, in Figure 7, a cyclonic formation moving to the south-southeast was marked by its periphery, then on 19 August 1987 in Figure 3, it was already identified by its central part: the core of the disturbance is clearly visible in the

section plane. In the period 9–19 August 1987, the SST in the south of the section increased by several degrees, which is apparently due to the advection of water from the south. Thus, the temperature at the test site has a complex spatiotemporal structure typical for the subarctic front zone. The front in the upper ocean layer has two branches: the northern one formed by the southern boundary of the Kuril (Subarctic) Current, and the southern one, which is the northern boundary of the transformed waters of the Kuroshio northern branch.

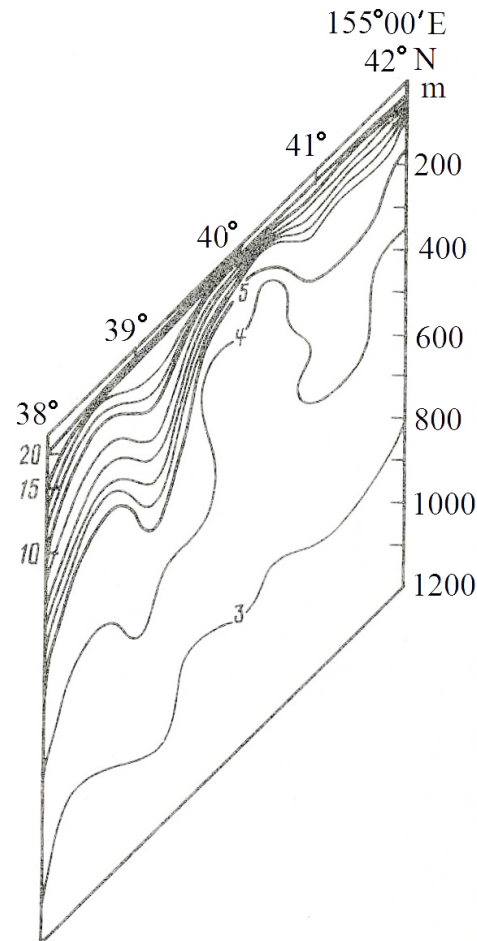


Figure 7. Vertical section of the temperature (in °C) made along the meridian 155°00' E on 9 August 1987. Adaptation of Figure 6 from [31].

Instrumental observations of currents at the Megapolygon were carried out from August to October 1987. Currents were measured at levels 120, 400, 1200 and 4500 m. Of the 186 autonomous buoy stations (ABS) installed at the test site, information came from 139 ABSs. Part of the ABSs was lost, and in other cases either the devices were torn off or their failures were observed. As an example, Figures 8–10 show the results of the average currents measured at the test site over the level of 120 m for August, September and October 1987. Let us pay attention to the field of average currents at 120 m in August 1987 (Figure 8). An element of randomness in the currents is introduced by the fact that the averaging interval was determined by the operating time of the velocity meter, and it was different.

However, in Figure 8, as in Figure 4, the Kuril (Subarctic) Current can be detected. In the central part of the polygon, it should also be noted that there is an anticyclonic disturbance, which is associated above with the transformation of the northern Kuroshio jet waters. Cyclonic disturbance centred at coordinates 40°00' N, 155°00' E is, apparently, the same one that stands out in Figures 3–5 and 7. A joint analysis of the temperature and currents allows one to draw a conclusion about their agreement.

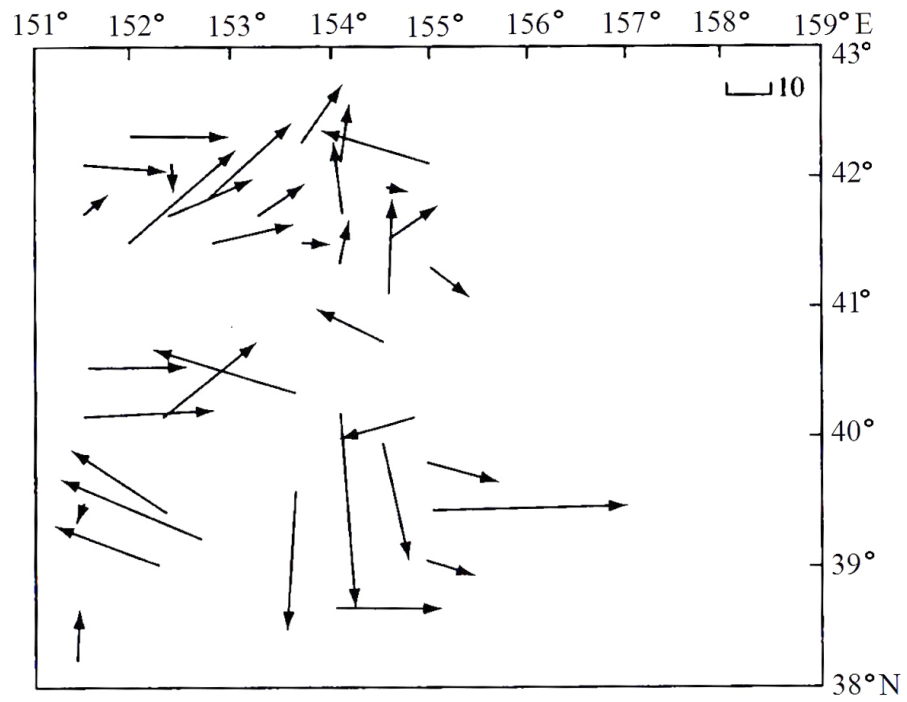


Figure 8. Average currents (in cm/s) at 120 m in August 1987. The arrow scale is at the upper right corner of the figure. Adaptation of Figure 15 from [32].

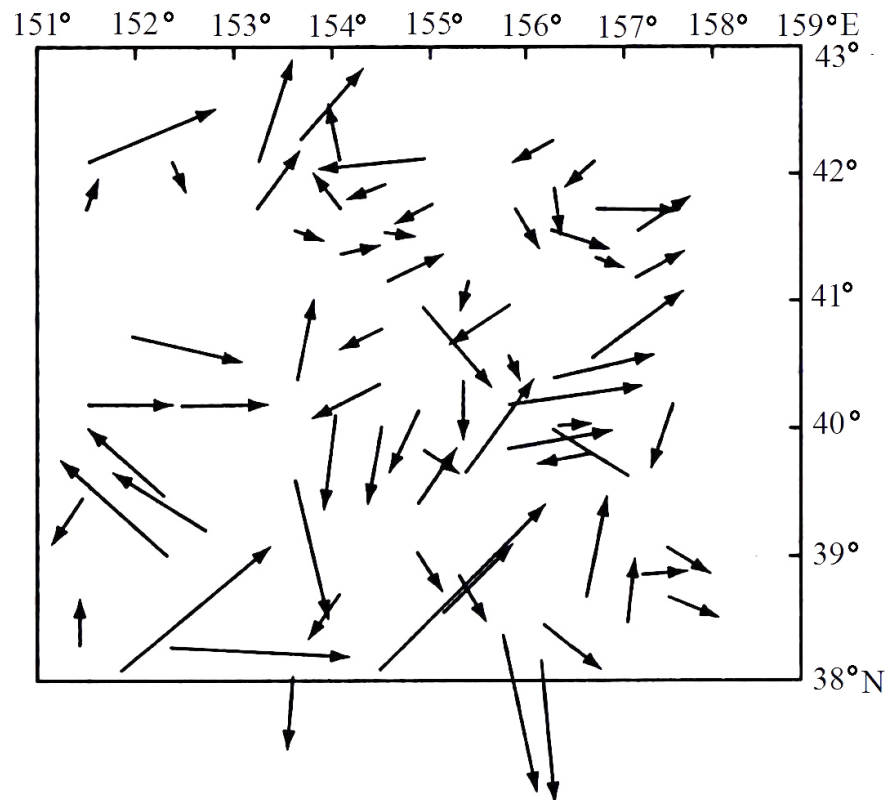


Figure 9. Average currents (in cm/s) at 120 m in September 1987. The arrow scale is at the upper right corner of the figure. Adaptation of Figure 16 from [32].

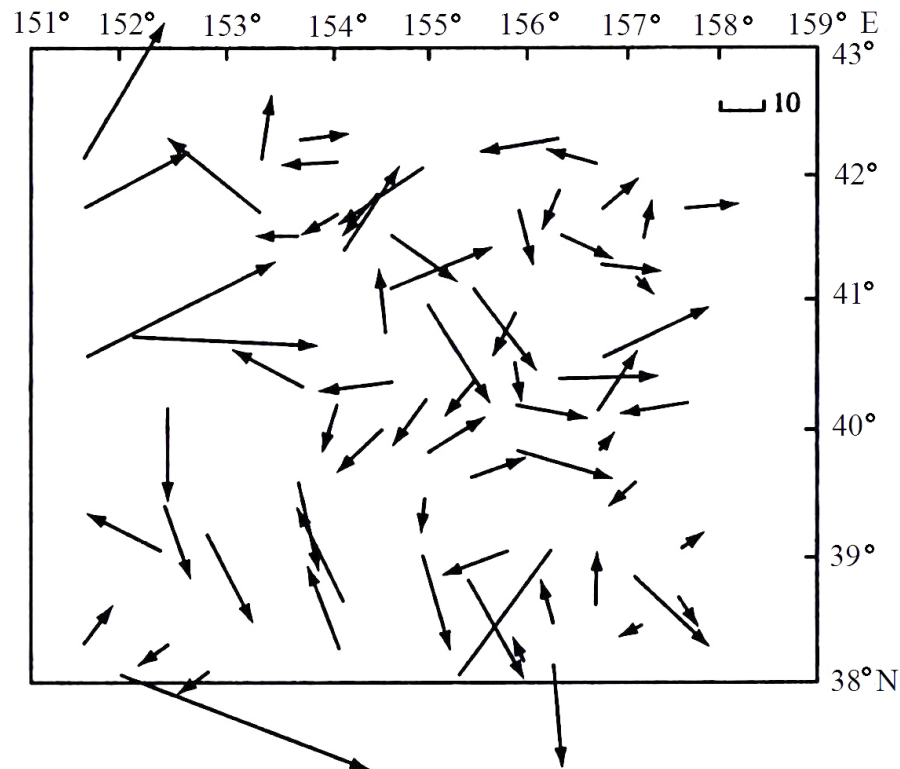


Figure 10. Average currents (in cm/s) at 120 m in October 1987. The arrow scale is at the upper right corner of the figure. Adaptation of Figure 17 from [32].

An analysis of current maps constructed by instrumental measurements at the test site allows us to establish a two-layer structure: eastern transport in the upper (120 and 400 m) and western transport in the deep (1200 and 4500 m) layers of the ocean. The structure and variability of the currents in the upper layer are characterized by a number of features [22].

1. The largest-scale elements of the currents, including the deep anticyclonic meander of the Subarctic Current (SAC) (Figure 4, 153–155° E), cyclonically vorticed currents of subarctic water to the west and east of this meander, and the three large anticyclonic Kuroshio rings of different ages in the southern half of the test site were very stable and observed throughout the entire observation time.
2. Temporal variability of the large-scale current pattern was associated with the deepening and weakening of the SAC anticyclonic meander, movements of its axis, movements of the Kuroshio anticyclonic rings, and displacements of individual jets.
3. The spontaneous intensification of individual SAC jets was accompanied by meandering and the separation of individual meanders and their transformation into cyclonic and anticyclonic eddies of synoptic scale.
4. A process is presently driven by the mesoscale exchange of water, heat and salt between eddies and the surrounding ocean. It is this process that leads to the final heat and salt exchange between the subarctic and interfrontal water masses across the subarctic front (SAF) associated with the generation of eddies.
5. Formation of the two types of eddies—rings and open ocean vortices—is caused by the same mechanism, which is baroclinic instability of large-scale currents.
6. The effect of a latitudinal change in the Coriolis parameter manifested in the movement of vortex disturbances in a westerly direction, was observed only for relatively weak and large eddy formations.

In the deep ocean (1200 and 4500 m), at the test site, the structure and variability of the currents were characterized by the following features [33].

1. The eastern SAC is not visible in the deep layer. Maps of currents at 120 m show the predominance of westerly currents. We can speak with fairly high confidence on the presence of a large-scale countercurrent under the SAC with an interface between these currents at a depth of about 1000 m.
2. All the largest synoptic disturbances of the currents in the thermocline [22] can be observed on maps for the level of 1200 m.
3. The small eddy formations observed in the thermocline (70–80 km) are not visible in the deep layer. At the same time, large non-stationary structural elements of circulation are observed in the deep ocean but are not present at the level of 1200 m. These include anticyclonic and cyclonic jets of currents with a width of 60–70 km. A powerful vortex formation with meridional and zonal dimensions of about 150 and 240 km, respectively, with an orbital movement of water of 20 cm/s at a level 1200 m, which appeared in October 1987, demonstrated a westward displacement with a speed of about 7 km/day.
4. The observation results made it possible to confirm the assumption of the presence of a western deep countercurrent under the SAC, which increases its speed with depth: it was higher at the 4500 m level than at the level of 1200 m

An analysis of hydrological observations and measured currents revealed the following features of the structure and variability of the currents in the deep ocean compared to ones in the thermocline. Some of the synoptic disturbances of the oceanic circulation covered the entire thickness of the ocean, while other ones were concentrated either only in the thermocline or only in the deep layer. The currents in the deep layer were characterized by significantly larger horizontal scales compared to ones in the thermocline. An analysis of current maps of high time resolution in the thermocline and in the deep ocean allows us to note that, in the latter, currents are significantly more non-stationary.

The processes of vortex formation observed at the “Megapolygon-87” in a wide range of spatiotemporal scales, transfrontal exchange, sudden and rapid changes in currents, temperature, salinity, and various hydrometeorological characteristics are undoubtedly associated with baroclinic and hydrodynamic instability of large-scale currents. Naturally, the structure and intensity of the ocean–atmosphere interaction in the region are formed with the participation of the ocean and reflect its current thermodynamic state. The results of heat budget assessments on the ocean surface (based on observations of hydrometeorological conditions in the test site area by 11 RVs) [34] turned out negative (in the warm half of the year!), which indicated a cooling of the ocean AUL. This was facilitated by both anomalous sensible and latent heat fluxes from the ocean to the atmosphere, abundant cloud cover reducing the short-wave solar radiation influx to the ocean surface, and active transfrontal exchange of warm central and cold polar waters, as previously reported. Anomalous cooling of waters in the region under consideration at the end of the 1980s was also noted in ([9], Figure 3).

3.2. The Experiment “Atlantex-90”

The hydrophysical interdepartmental experiment “Atlantex-90” [23,35] was carried out from November 1989 to June 1990 in the northwestern part of the AO (35°00′–55°00′ N, 60°00′–25°00′ W). The purpose of this experiment was an intensive, comprehensive study of the Gulf Stream system. The following RVs took part in the hydrological surveys and comprehensive observations of the thermodynamic state of the Gulf Stream—NA Current system: the weather RVs “Viktor Bugaev” (voyage 54); “Musson” (voyages 61 and 62); “Volna” (voyages 51 and 52); RVs IO RAS “Vityaz” (voyage 19); “Professor Stockman” (voyage 26); “Akademik Kurchatov” (voyage 50); scientific and fishing vessel PINRO “Persey-III”. The experiment allowed us to obtain important evidence on the features concerning the thermodynamic state of the system Gulf Stream—NA Current, large-scale and synoptic dynamics of the ocean and its interaction with the atmosphere, and the evolution of atmospheric pressure formations over the ocean in the climate phase characterized by the WO thermal discharge (1975–1999) [4].

Consider some results obtained in the scope of the experiment “Atlantex-90”. Figure 11 presents (a) a fragment of the subpolar front separating the Labrador and Central Atlantic water structures, and (b) the position and dynamics of the front on the ocean surface for 22–29 June 1990 in the region $48^{\circ}00'–52^{\circ}00' S$, $45^{\circ}00'–36^{\circ}00' W$. The frontal section of the above-mentioned structures is visible from the surface to depths of 1200–1500 m (isotherms 4–8 °C). In the layer 500–1000 m, to the right of the front, an intrathermoclinic lens is observed, which is the core of an intrathermoclinic anticyclonic vortex [36]. The detailed structure of the lens and some of its hydrophysical characteristics on a section along $48^{\circ}00' N$ are presented in Figure 12.

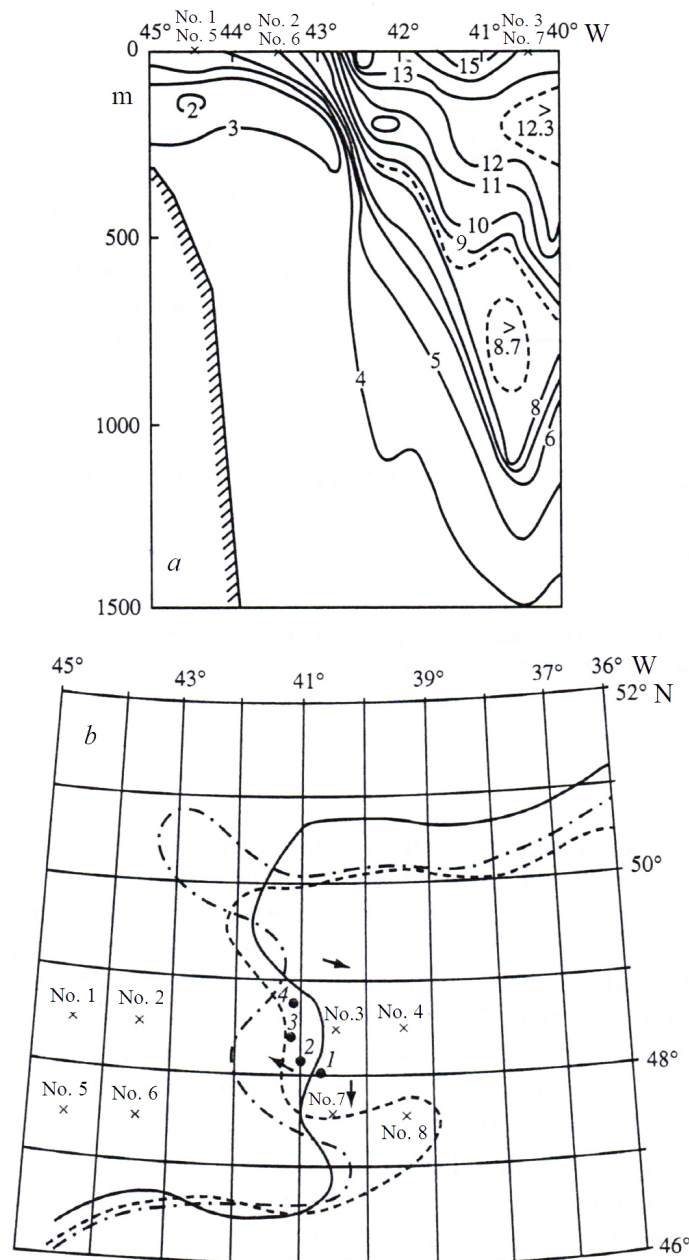


Figure 11. (a) Zonal (along $48^{\circ} N$) temperature section made on 13–15 June 1990 by the RV “Akademik Kurchatov” (voyage 50), and (b) the position of the isotherm $12^{\circ} C$ on the ocean surface on 22–29 June 1990 presenting the front location. The points indicate the position of the “AK-50” lense centre for different dates: 1–16 June, 2–25 June, 3–28 June and 4–30 June 1990; crosses mark the centres of one-degree squares No. 1–8. Solid, dashed and dash-dot lines represent the front dynamics for 22–29 June 1990. Arrows indicate the measured currents. Adaptation of Figure 61 from [32].

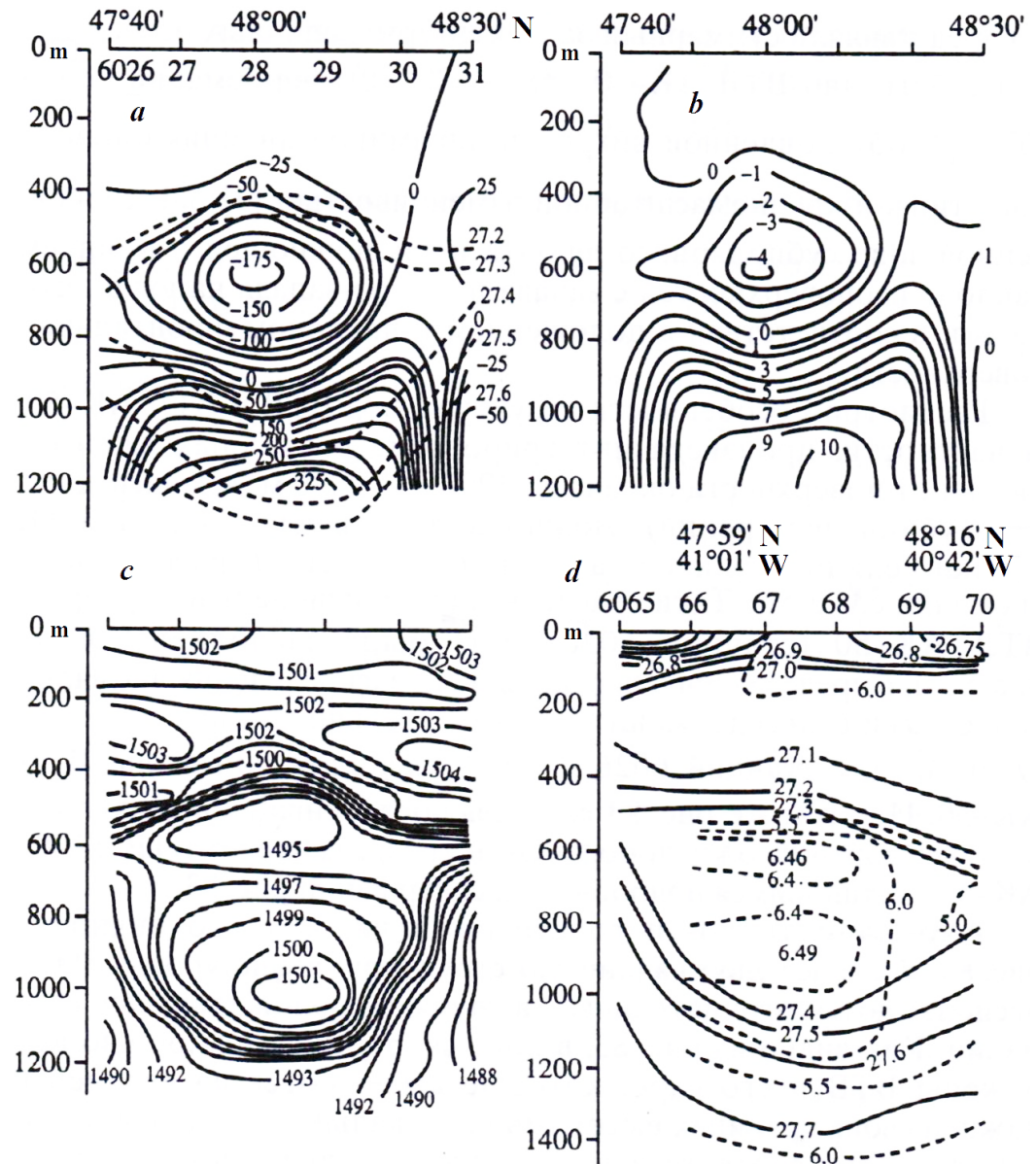


Figure 12. Distribution of (a) anomalies of heat content (in 10^7 J/m²), (b) salt content (in 10^{-1} kg/m²), (c) sound speed (in m/s) and (d) oxygen (in mL/l) at a section through the lens. The dashed line shows the isopycnals in (a) and the oxygen distribution in (d). On the upper scale (a–c), position of the stations 6026–6031 is marked (from left to right), and on (d)—stations 6065–6070. Adaptation of Figure 83 from [32].

An important question is the nature of the lens and the intrathermocline vortex (ITV). Through numerical modelling, using a differential-parametric model of the upper layer of the ocean [37], the hypothesis was confirmed [38] (Figure 13), in that the mechanism of their generation was deep winter convection. In particular, the modelling made it possible to determine the area of the ITV formation (on the eastern periphery of the subpolar front), as well as the conditions and time: in February 1990, during the invasion of cold, moisture-deficient Arctic air masses to the subpolar front area.

The presence of an intrathermocline lens and ITV indicates an intensification of vertical exchange with heat and salt, as well as other oceanological characteristics between the surface and deep layers. Estimates of anomalies in heat, salt and oxygen content in the main thermocline layer caused by local convective process amounted to 3.82×10^{19} J, 8.05×10^{11} kg and 4.65×10^{12} L, respectively.

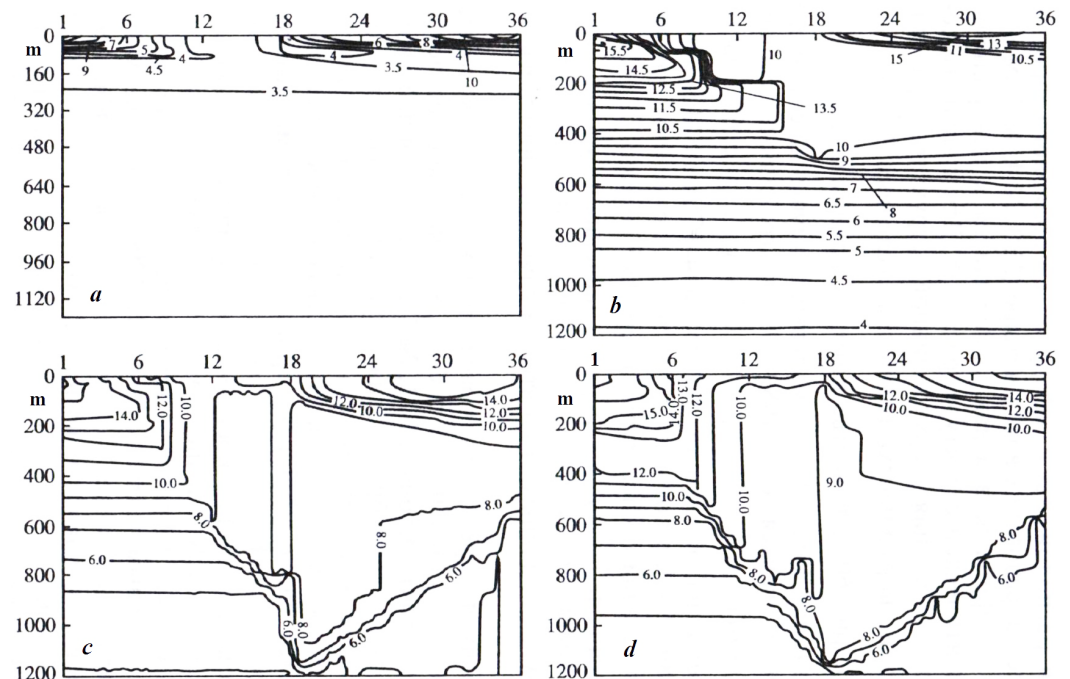


Figure 13. Evolution of the thermal structure at points (a) N1 and (b) N4 under boundary conditions $T_{z=0}(t) + \delta T(t), S_{z=0}(t), V_{z=0}(t)$; at points (c) N4 and (d) N8 under boundary conditions $T_{z=0}(t) + \delta T(t), S_{z=0}(t) + \delta S(t), V_{z=0}(t)$. Horizontal time scale means: 1 is the first 10 days of September, etc. Adaptation of Figure 63 from [32].

In May–June 1990, two ships of the Shirshov Institute of Oceanology (“Vityaz” and “Professor Stockman”) carried out two consecutive hydrophysical surveys (02–22 May 1990 and 27 May–10 June 1990) with high spatial and temporal resolution of the Gulf Stream delta region: $37^{\circ}00'–42^{\circ}30' N, 42^{\circ}00'–49^{\circ}00' W$. The most remarkable element of the water structure was the presence, according to the results of the first survey of a cyclonic meander of the Gulf Stream (Figure 14) with the capture of polar waters, which emerged as an independent formation according to the results of the second survey. Using the results of isopycnal analysis, estimates were made of the Labradorian waters volume and the associated heat and salt deficits arising on the eastern flank of the Gulf Stream due to episodic transfrontal transport. The orders of these quantities turned out to be as follows: $6.11 \times 10^3 \text{ km}^3$ for the water volume, $28.4 \times 10^{18} \text{ J}$ for heat, $1.65 \times 10^{12} \text{ kg}$ for the salt mass.

The period of research in the scope of the programme “Atlantex-90” was characterized by the complex structure of the frontal zone and intense eddy dynamics of the Gulf Stream system region [39]. In contrast to eddies of convective nature ITV and rings caused by transfrontal exchange (hydrodynamic instability of the front), the main source of eddies in the open ocean is the baroclinic instability of large-scale currents. Let us consider three successive meridional (along $36^{\circ} W$) sections of the NA Current hydrological structure (Figure 15) measured with the device CTD (Conductivity, Temperature and Depth). The top of Figure 15 shows the SST. Its analysis reveals the presence of the two frontal zones: near $51^{\circ}00' N$ and between 48° and $49^{\circ} N$. Maximum temperature and salinity gradients are observed at a depth 200 m, and for these elements, they are higher here than on the surface. The southern front is noticeably deeper and more pronounced than the northern one, but not on the surface, where the temperature difference ($2–3^{\circ} C$) was smaller than in the area of the northern front ($4–5^{\circ} C$).

In the upper layers, the northern front is well tracked by the isohaline 35.0 PSU, which is usually taken [40] as a boundary between the Labrador Sea and intermediate waters. This isohaline plunges from north to south, showing, this way, their distribution in this direction under intermediate waters. The southern front is well marked by the isohaline 35.5 PSU, which separates the intermediate water from the NA central one. On all the three sections along 36° W, the position of the northern front coincides with the eastward direction of geostrophic flows (Figure 15). In the core of this stream, the current velocity varied from more than 30 cm/s in the period 29 May–7 June to 12.5 cm/s in the period 18–24 June. Similarly, the easterly flow in the area of the southern front in these sections can be interpreted as the southern branch of the NA current. Dynamic velocities varied from 30 to 50 cm/s.

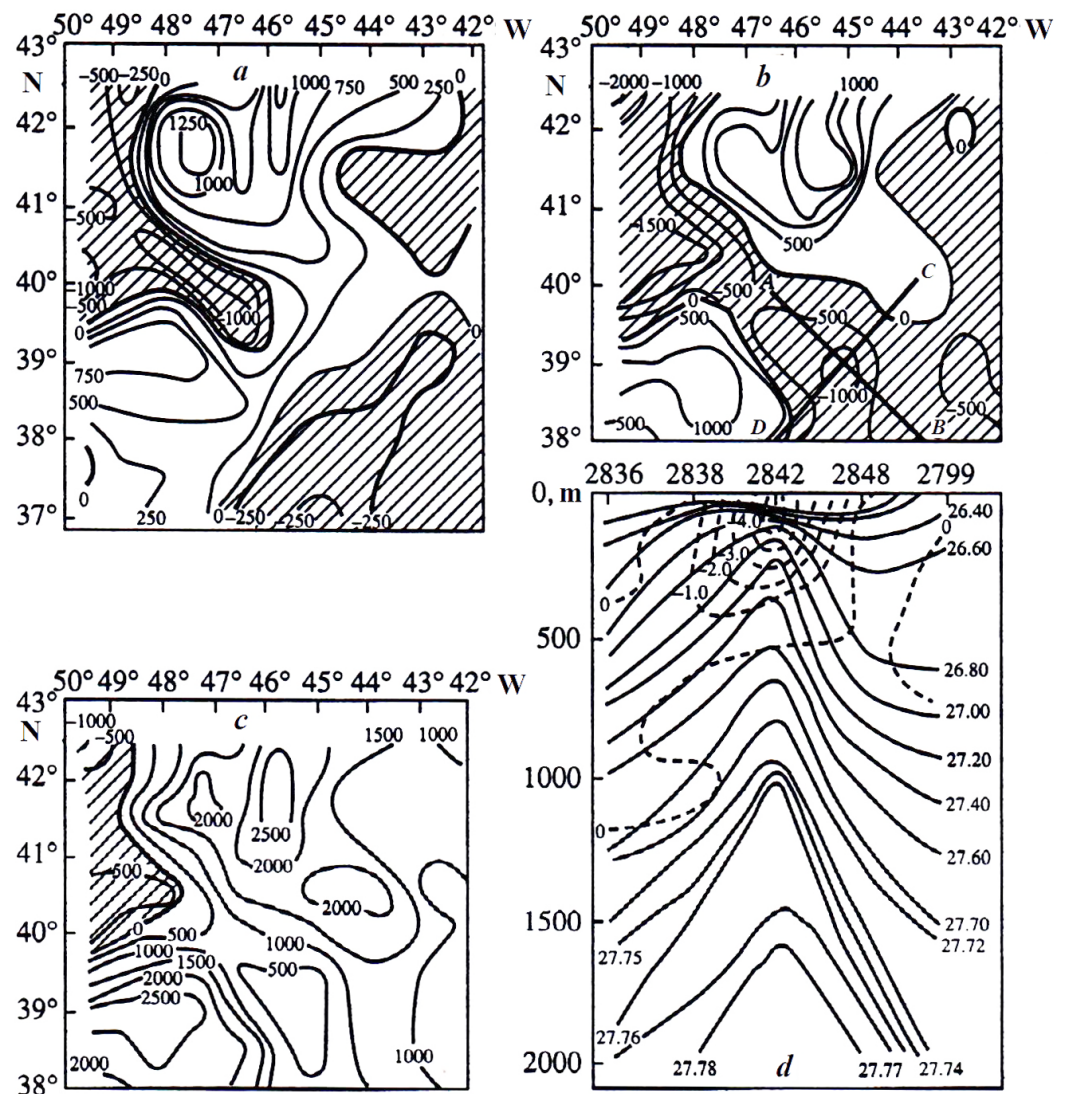


Figure 14. Anomalies of the heat content in the Gulf Stream delta waters for the layers (a) 0–500 m, (b) 0–1000 m and (c) 0–2000 m, and (d) isopycnal temperature anomalies on the normal (b), line AB to the section front across the ring. CD is the ring section parallel to the front. Adaptation of Figure 85 from [32].

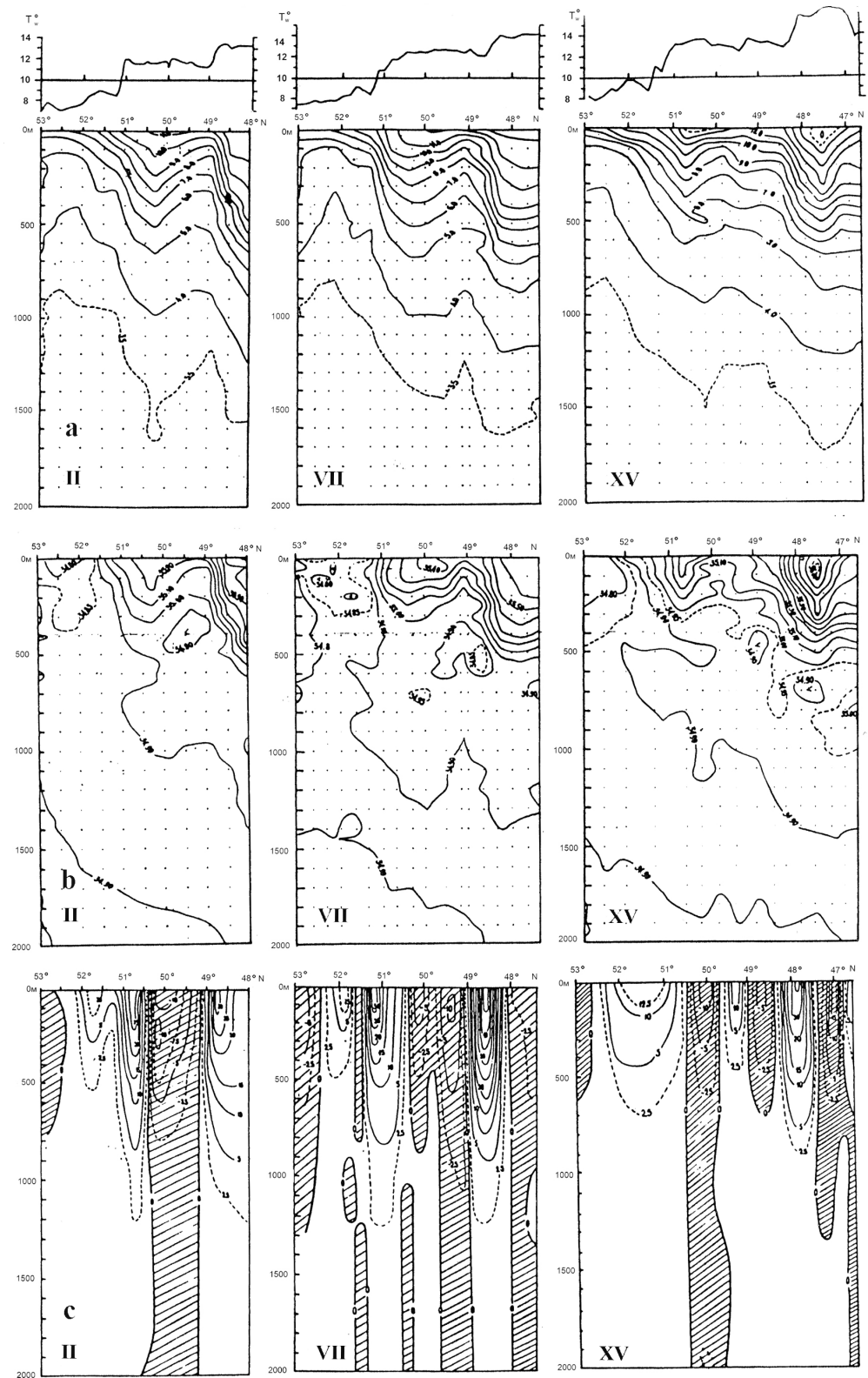


Figure 15. Results of hydrological observations on (II) 22–23 May, (VII) 29 May–7 June and (XV) 18–24 June CTD columns on sections along the meridian 36° W. T_w is SST, (a) is water temperature, (b) is salinity, (c) is dynamic velocity (cm/s). The dashed line shows currents directed out of the figure. A depth of 2000 m was chosen as the reference level for dynamic calculations. SST on sections was obtained by averaging several sections during the installation and inspection of buoys. Adaptation of Figure 4 from [39].

Instrumental observations of currents in the experiment “Atlantex-90” were carried out from 31 May to 23 June 1990 on a meridional section along 36° W between 47° and 53° N. The currents were measured at horizons 100, 400, 1000, 2000 and 3500 m. Hodographs of the velocity vectors for the measured currents averaged over the observation period for 14 buoy stations on the meridian 36° W are presented in Figure 16 and are in good agreement with geostrophic flows on this section (Figure 15).

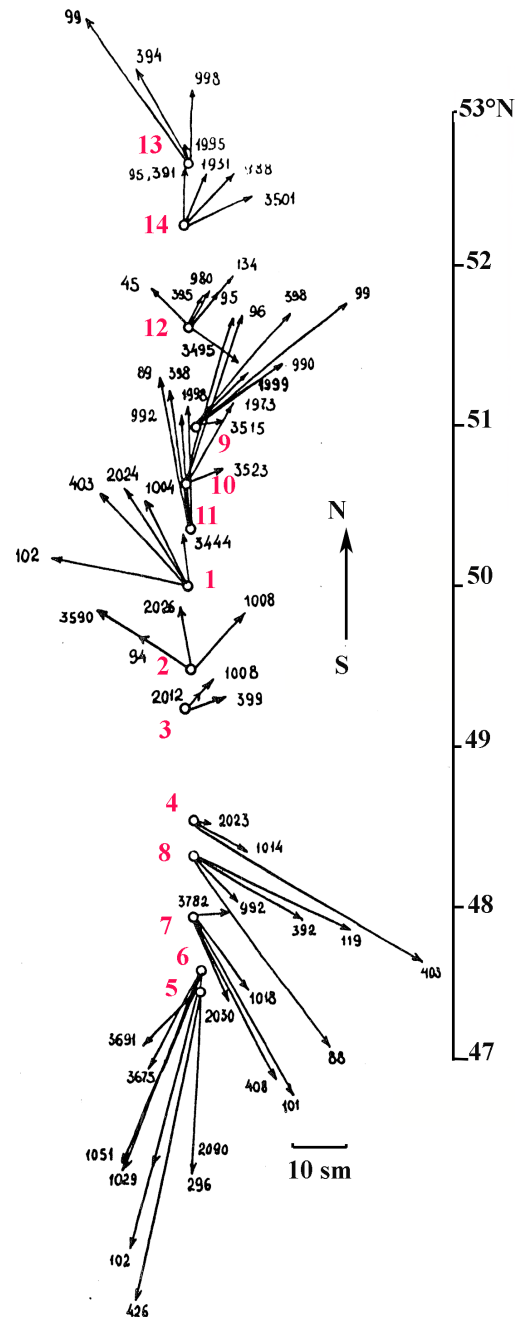


Figure 16. Hodographs of current velocity vectors averaged over the observation period for 14 buoy stations on the meridian 36° W. Adaptation of Figure 14 from [39].

Figure 17 shows the structure of flows on the meridian 36° W according to instrumental observations for 6, 11 and 16 June 1990, as well as for the entire observation period. The main zonal flows (two eastern and three western) cover the entire thickness from 100 to 3600 m. The highest current velocities were observed in the upper layers (100 and 400 m). They decreased with depth, but, in some places, they increased somewhat again in the

bottom layer. Distribution of the meridional component of currents on individual days and when averaged over the observation period shows the presence of large-scale divergence with northern flows in the northern part of the section and southern ones in its southern part (Figure 17). There is also a certain tendency towards the formation of a two-layer meridional circulation, with flows at the bottom opposite in direction to the rest of the water column.

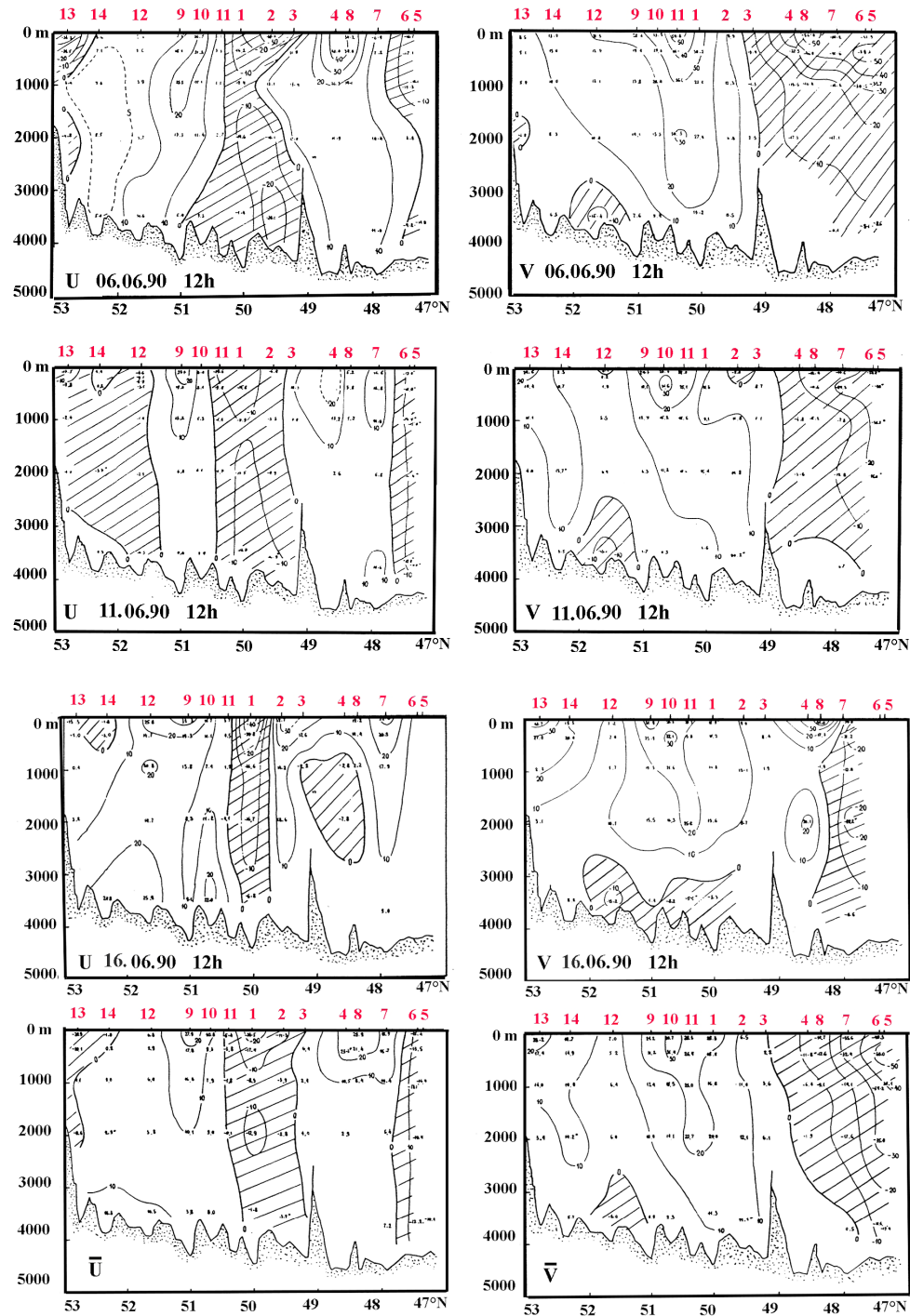


Figure 17. Zonal (u) and meridional (v) components of current velocity according to instrumental observations for 6, 11 and 16 June 1990, as well as averages for the entire observation period. Asterisks at some average values of current velocity components indicate that they were brought to a full range of observations by comparison with observations at neighbouring horizons. Adaptation of Figure 16 from [39].

4. Discussion

Large-scale hydrophysical experiments “Megapolygon” (subarctic frontal zone of the northwestern PO, July–October 1987) and “Atlantex-90” (Newfoundland energetic zone, May–July 1990) were carried out in the two key areas of the WO during the multidecadal rhythm of the present-day climate (1940–1999). Unprecedented observations during the implementation of these two projects made it possible to obtain extremely important comprehensive instrumental evidence of thermodynamic processes during multidecadal oscillation of the heat content of the WO during the phase of its thermal discharge (1975–1999) [4,5]. These observations made it possible to establish the characteristic anomalous thermodynamic states of the named water areas.

In particular, based on the observational data in these experiments, the following results were obtained.

1. The formation of large-scale SST anomalies was studied in the PO [34,41] and AO [42].
2. Signs of extreme volume transport in the Labrador Current (based on the anomalously low water temperature in its core, $-1.2\text{ }^{\circ}\text{C}$) and the NA Current on the meridional section at 36° W (up to 100 Sv) were identified [43].
3. The intensification of transfrontal water transport has been established both on the subarctic front in the PO [32] and on the subpolar front in the AO [44].
4. High fluxes of sensible and latent heat from the ocean to the atmosphere were determined [30,45], and as a result, abnormally developed cloud covers were discovered in the water areas of each experiment.
5. Facts of winter deep density convection have been recorded [27,38].

The climate shifts that have occurred over the past 100–150 years [3] were obviously phase transitions of the climate system from a state of heat accumulation by the WO AUL (the layer of the main thermocline) to a state of thermal discharge of this layer. As observations have shown, the thermal discharge phase occurs through heat exchange between the ocean AUL and the atmosphere with the participation of deep-density convection (Figures 11–13) and the process of transfrontal exchange of polar and central oceanic waters in the PO (Figures 3–7) and in the AO (Figure 14). Demonstration of deep convection on the subpolar front in the NA during the cold season 1989–1990 was the generation of an intrathermoclinic lens (ITL) discovered and studied during the experiment “Atlantex-90” (voyage 50 of the RV “Akademik Kurchatov”). The ITL was located in a layer 500–1000 m and had a horizontal size of about 100 km. Estimates of anomalies in heat and salt content, as well as oxygen content in the ITL (Figure 12) were $3.82 \times 10^{19}\text{ J}$, $8.05 \times 10^{11}\text{ kg}$ and $4.65 \times 10^{12}\text{ L}$, respectively.

The vertical distributions of phosphates and oxygen measured at stations 6062, 6066 and 6068 (Figure 84 in [32]) located on a zonal section through the ITL (Figure 12d) made it possible to establish its difference in hydrochemical characteristics from Mediterranean lenses, despite their multiple analogues: anomalies in temperature, salinity, density, etc. Apparently, earlier in the experiment “Topogulf” [46] products of frontal lens destruction, similar to what we discovered in “Atlantex-90”, were observed, rather than Mediterranean ITL, as previously assumed [47]. The zonal section of water temperature (along 48° N) is given in Figure 11. This section shows (a) the subpolar front and the ITL, (b) the position and dynamics of the front, as well as the ITL relative to it. Modelling of the thermal structure evolution (Figure 13) made it possible to establish the nature of ITL (deep density convection), the time and location (in February–March 1990 on the eastern periphery of the subpolar front) of its formation.

The features and nature of multidecadal changes of the Northern Hemisphere (NH) atmospheric circulation in the present era can be understood based on Dzerdzeevskiy’s diagnosis of a secular series of atmospheric circulation types [48–50]. Temporal changes in individual pairs of atmospheric circulation groups are shown in Figure 18. In particular, it shows changes in zonal (1 + 5) and meridional southern (3 + 10 and 4) circulation types. The balance ratios of the meridional southern (3 + 10) and northern (2 + 6) atmospheric

circulation groups of the NH are shown in Figure 19. Noteworthy is the alternation of multidecadal northern and southern phases of atmospheric circulation types over the oceans and continents (curves 1, 2 and 4 in Figure 19). It is important to note that, during the multidecadal phase of increasing the frequency of northern meridional processes over the oceans, their reduction over the continents is observed, and, during the same phase, the frequency of southern processes decreases over the oceans and increases over the continents.

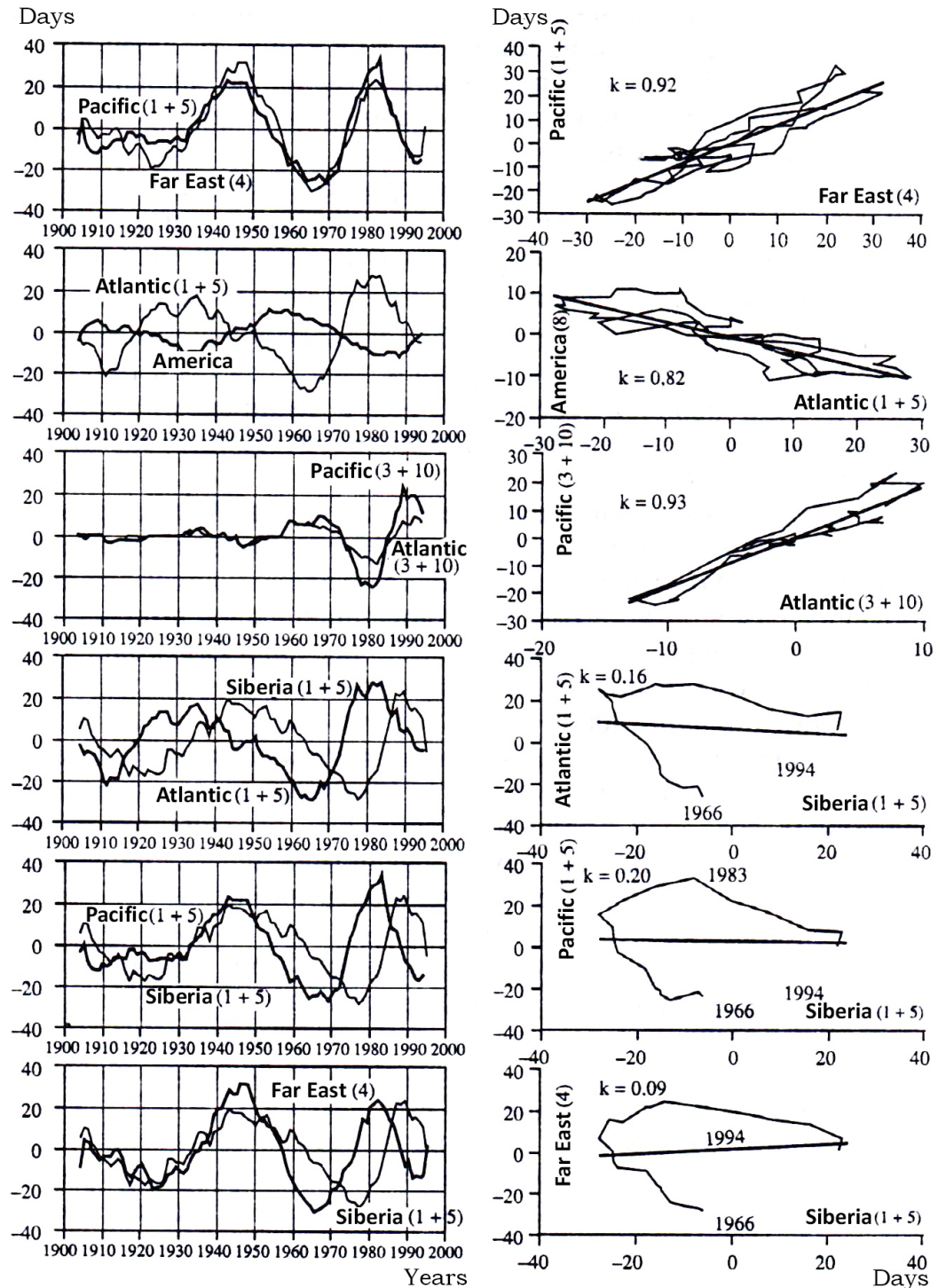


Figure 18. (Left) cyclic components of individual pairs of atmospheric circulation groups: (1) zonal western, (3) meridional southern, (4) meridional southern and western, (5) zonal western and stationary, (10) meridional southern and stationary; (right) their amplitude-phase diagrams, k is correlation coefficient for these pairs. Adaptation of Figure 110 from [32].

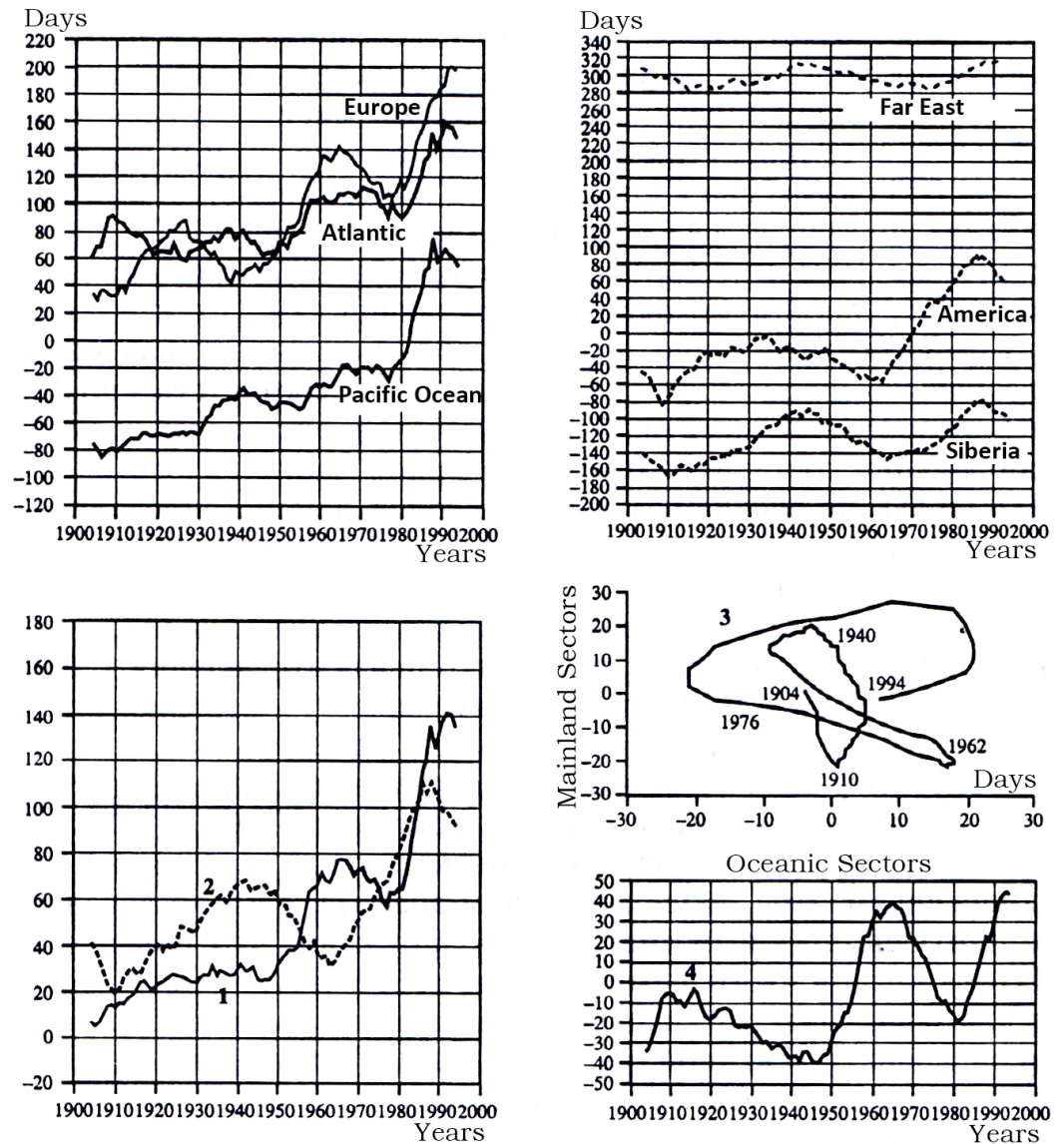


Figure 19. Changes in the balance of meridional southern (1 + 5) and northern (2 + 6) atmospheric circulation groups for (top) different sectors of the NH and (bottom) for oceans and continents: 1 marks oceans, 2 marks continents, 3 marks amplitude-phase diagrams of cyclic oscillations and 4 marks the difference between oceans and continents (between curves 1 and 2). Adaptation of Figure 111 from [32].

For the climatic phases of heat accumulation by the WO (1940–1974 and 2000–2022), one should expect a noticeable weakening of such processes as deep density convection, transfrontal exchange of polar and central oceanic waters, sensible and latent heat fluxes from the ocean to the atmosphere, transition of available potential energy into a kinetic one accompanied by an intensification of eddy activity in the ocean. Analysis of the multi-decadal atmospheric circulation structure variability in the NH made it possible to identify its important features (Figures 18 and 19). As an example for the XX century, Figure 18 shows some multidecadal structures (zonal western (1 + 5) and meridional southern (3 + 10) types) of atmospheric circulation in the six sectors of the NH. Noteworthy is the connectivity and uniformity of the atmospheric circulation in some sectors of the NH: the PO (1 + 5) and the Far East (4), the PO and AO (3 + 10), but its multidirectionality takes place in other sectors: Atlantic (1 + 5) and American (1 + 5), PO (1 + 5) and Siberia (1 + 5), Far East (4) and Siberia (1 + 5). The balances of the meridional southern and northern groups of atmospheric circulation (Figure 19) reflect significant differences for the oceanic and

continental sectors (curves 1, 2 and 4). The oscillatory multidecadal nature of a certain balance in the atmospheric circulation obviously indicates the presence of self-oscillations in the ocean–atmosphere–continent climate system that have the structure of standing waves. Such a regime is probably a demonstration of the system’s tendency to preserve the integral angular momentum of the atmosphere [51].

5. Conclusions

Multidecadal climate shifts, which have occurred sporadically over the past 100–150 years, should be considered the most significant feature of the dynamics of present-day climate. There is reason to believe that these phenomena will be observed in the near future. In the mid-1970s, for the first time, attention was drawn to sudden rapid climate changes, which were referred to as “climate shifts”. The scientific community was not ready to perceive these phenomena as a natural behaviour of the climate system. It took some time to understand that this is a global, rather than regional, phenomenon, and that behind it is WO, namely, a change in the thermodynamic regime of its AUL (0–1000 m). As characteristics of the thermodynamic state of the WO AUL, it is advisable to consider processes such as sensible and latent heat fluxes from the ocean to the atmosphere accompanied by the formation of a cloud cover that screens the shortwave solar radiation income to the ocean surface; deep density convection, which determines the thickness of the near-surface oceanic layer interacting with the atmospheric boundary layer; transfrontal exchange of cold and freshened polar waters with warmer and saltier central ocean waters; hydrodynamic and baroclinic instability of large-scale WO currents and, naturally, such systems as the Kuroshio and Gulf Stream, the Antarctic Circumpolar Current, etc.; the transition of available potential energy into a kinetic one, the result of which is the generation of vorticity; formation of positive and negative thermal anomalies in the ocean.

Unprecedented data on thermodynamic processes in the ocean during the climatic phase of its thermal discharge (1975–1999) were obtained during the implementation of the projects Megapolygon [30] (PO, 1987) and Atlantex-90 [23] (AO, 1990) in areas of current systems Kuroshio and Gulf Stream, respectively. The materials of these experiments made it possible to obtain important factual information about each of the above processes, thereby confirming their validity and assessing their significance. Thus, an important feature of the present-day climate is the presence of a sequence of relatively continental and humid phases (25–35 years each) of global climate. Phase transitions from a continental phase to a humid one occur rapidly (for 2–3 years) and are accompanied by qualitative changes, and, therefore, are considered “climatic shifts”. It has been established that the WO has phases of heat accumulation and heat discharge, the first of which corresponds to the continental climate, and the second one concerns increasing its humidity. As a result of the WO thermohydrodynamic numerical modelling, signs of the heat content planetary oscillation localized in the layer of its main thermocline were identified. Since the main thermocline layer is the one where the most important elements of the WO circulation are located, the idea arose to verify (based on observational data) the uniformity of the thermodynamic regime in two key current systems—the Kuroshio and the Gulf Stream—during the thermal discharge phase. The study carried out allows us to conclude that, during the phase of the WO thermal discharge (1975–1999), both current systems were in the following similar thermodynamic conditions.

1. Increased sensible and latent heat fluxes from the ocean to the atmosphere were observed.
2. The transfrontal exchange of subpolar and subtropical waters was intensified.
3. Deep density convection took place.
4. Eddy activity in each of the regions was high.

The lack of large-scale experimental data in a number of key WO areas during various climate phases creates certain limitations in solving emerging problems. Prospects for the development of research in the context of a shortage of necessary information are expected to test a number of working hypotheses using indirect data.

Author Contributions: Conceptualization, V.B.; methodology, V.B.; software, A.G. and A.S.; validation, V.B., A.G. and A.S.; formal analysis, V.B.; investigation, V.B.; resources, V.B.; data curation, V.B. and A.G.; writing—original draft preparation, V.B. and A.S.; writing—review and editing, A.G.; visualization, A.S.; supervision, V.B. All authors have read and agreed to the published version of the manuscript.

Funding: The research was funded by the Russian Science Foundation (grant no. 22-17-00267) in the field of ocean model development and numerical simulations and by federal assignment to the Shirshov Institute of Oceanology RAS (subject no. FMWE-2024-0017) in the field of data analysis and investigation.

Institutional Review Board Statement: Not applicable.

Informed Consent Statement: Not applicable.

Data Availability Statement: Data are contained within the article.

Conflicts of Interest: The authors declare no conflicts of interest.

Abbreviations

The following abbreviations are used in this manuscript:

ABS	Autonomous Buoy Station
AO	Atlantic Ocean
AUL	Active Upper Layer
CMIP	Coupled Model Intercomparison Project
CORE	Coordinated Ocean–Ice Reference Experiment
CTD	Conductivity, Temperature and Depth measuring device
GAO	Global Atmospheric Oscillation
INMOM	Institute of Numerical Mathematics Ocean Model
IPCC	Intergovernmental Panel on Climate Change
ITL	IntraThermocline Lense
ITV	IntraThermocline Vortex
MOHO	Multidecadal Oscillation of the Heat content in the Ocean
NA	North Atlantic
NH	Northern Hemisphere
OGCM	Ocean General Circulation Model
OMIP	Ocean Model Intercomparison Project
PO	Pacific Ocean
RV	Research Vessel
SAC	SubArctic Current
SAF	SubArctic Front
SRT	Ship-based Remote Thermometer
SST	Sea Surface Temperature
WBC	Western Boundary Currents
WO	World Ocean

References

- Bond, N.; Overland, J.; Spillane, M.; Stabeno, P. Recent shifts in the state of the North Pacific. *Geophys. Res. Lett.* **2003**, *30*, 2183. [[CrossRef](#)]
- Byshev, V.; Neiman, V.; Romanov, Y.; Serykh, I. Phase variability of some characteristics of the present-day climate in the northern atlantic region. *Dokl. Earth Sci.* **2011**, *438*, 887–892. [[CrossRef](#)]
- Henley, B.; Gergis, J.; Karoly, D.; Power, S.; Kennedy, J.; Folland, C. A Tripole Index for the Interdecadal Pacific Oscillation. *Clim. Dyn.* **2015**, *45*, 3077–3090. [[CrossRef](#)]
- Byshev, V.; Gusev, A.; Neiman, V.; Sidorova, A. Interdecadal Oscillation of the Ocean Heat Content as a Contribution to Understanding of Physical Aspects of the Present-Day Climate. *J. Mar. Sci. Eng.* **2022**, *10*, 1064. [[CrossRef](#)]
- Byshev, V.; Neiman, V.; Anisimov, M.; Gusev, A.; Serykh, I.; Sidorova, A.; Figurkin, A.; Anisimov, I. Multi-Decadal Oscillations of the Ocean Active Upper-Layer Heat Content. *Pure Appl. Geophys.* **2017**, *174*, 2863–2878. [[CrossRef](#)]
- Byshev, V.; Neiman, V.; Romanov, Y.; Serykh, I.; Sonechkin, D. Statistical significance and climatic role of the Global Atmospheric Oscillation. *Oceanol.* **2016**, *56*, 165–171. [[CrossRef](#)]
- Kamenkovich, V., Monin, A. (Eds.) *Ocean Physics (in 2 Volumes), Vol.1: Ocean Hydrophysics*; Nauka: Moscow, Soviet Union, 1978; 455p.

8. Gill, A. *Atmosphere-Ocean Dynamics*; International Geophysics Series; Academic Press: Orlando, FL, USA, 1982; Volume 30; 680p.
9. Kwon, Y.O.; Alexander, M.; Bond, N.; Frankignoul, C.; Nakamura, H.; Qiu, B.; Thompson, L. Role of the Gulf Stream and Kuroshio–Oyashio Systems in Large-Scale Atmosphere–Ocean Interaction: A Review. *J. Clim.* **2010**, *23*, 3249–3281. [[CrossRef](#)]
10. Wallace, J.; Hobbs, P. *Atmospheric Science: An Introductory Survey*; Academic Press/Elsevier: Burlington, MA, USA, 2006; 483p.
11. Lappo, S.; Gulev, S.; Rozhdestvensky, A. *Large-Scale Thermal Interaction in the Ocean-Atmosphere System and Energy-Active Regions of the World Ocean*; Hydrometeoizdat: Leningrad, Soviet Union, 1990; 336p. (In Russian)
12. Griffies, S.; Biastoch, A.; Böning, C.; Bryan, F.; Danabasoglu, G.; Chassignet, E.; England, M.; Gerdes, R.; Haak, H.; Hallberg, R.; et al. Coordinated Ocean-ice Reference Experiments (COREs). *Ocean Model.* **2009**, *26*, 1–46. [[CrossRef](#)]
13. Danabasoglu, G.; Yeager, S.; Bailey, D.; Behrens, E.; Bentsen, M.; Bi, D.; Biastoch, A.; Böning, C.; Bozec, A.; Canuto, V.; et al. North Atlantic simulations in Coordinated Ocean-ice Reference Experiments phase II (CORE-II). Part I: Mean states. *Ocean Model.* **2014**, *73*, 76–107. [[CrossRef](#)]
14. Danabasoglu, G.; Yeager, S.; Kim, W.; Behrens, E.; Bentsen, M.; Bi, D.; Biastoch, A.; Bleck, R.; Böning, C.; Bozec, A.; et al. North Atlantic simulations in Coordinated Ocean-ice Reference Experiments phase II (CORE-II). Part II: Inter-annual to decadal variability. *Ocean Model.* **2016**, *97*, 65–90. [[CrossRef](#)]
15. Downes, S.; Farneti, R.; Uotila, P.; Griffies, S.; Marsland, S.; Bailey, D.; Behrens, E.; Bentsen, M.; Bi, D.; Biastoch, A.; et al. An assessment of Southern Ocean water masses and sea ice during 1988–2007 in a suite of interannual CORE-II simulations. *Ocean Model.* **2015**, *94*, 67–94. [[CrossRef](#)]
16. Farneti, R.; Downes, S.; Griffies, S.; Marsland, S.; Behrens, E.; Bentsen, M.; Bi, D.; Biastoch, A.; Böning, C.; Bozec, A.; et al. An assessment of Antarctic Circumpolar Current and Southern Ocean meridional overturning circulation during 1958–2007 in a suite of interannual CORE-II simulations. *Ocean Model.* **2015**, *93*, 84–120. [[CrossRef](#)]
17. Griffies, S.; Danabasoglu, G.; Durack, P.; Adcroft, A.; Balaji, V.; Böning, C.; Chassignet, E.; Curchitser, E.; Deshayes, J.; Drange, H.; et al. OMIP contribution to CMIP6: Experimental and diagnostic protocol for the physical component of the Ocean Model Intercomparison Project. *Geosci. Model Dev.* **2016**, *9*, 3231–3296. [[CrossRef](#)]
18. Tsujino, H.; Urakawa, L.; Griffies, S.; Danabasoglu, G.; Adcroft, A.; Amaral, A.; Arsouze, T.; Bentsen, M.; Bernardello, R.; Böning, C.; et al. Evaluation of global ocean–sea-ice model simulations based on the experimental protocols of the Ocean Model Intercomparison Project phase 2 (OMIP-2). *Geosci. Model Dev.* **2020**, *13*, 3643–3708. [[CrossRef](#)]
19. Solomon, S.; Qin, D.; Manning, M.; Chen, Z.; Marquis, M.; Averyt, K.; Tignor, M.; Miller, H. (Eds.) *Climate Change 2007: The Physical Science Basis. Contribution of Working Group I to the Fourth Assessment Report of the Intergovernmental Panel on Climate Change*; Cambridge University Press: Cambridge, UK; New York, NY, USA, 2007.
20. Stocker, T.; Qin, D.; Plattner, G.K.; Tignor, M.; Allen, S.; Boschung, J.; Nauels, A.; Xia, Y.; Bex, V.; Midgley, P. (Eds.) *Climate Change 2013: The Physical Science Basis. Contribution of Working Group I to the Fifth Assessment Report of the Intergovernmental Panel on Climate Change*; Cambridge University Press: Cambridge, UK; New York, NY, USA, 2013.
21. Masson-Delmotte, V.; Zhai, P.; Pirani, A.; Connors, S.; Pán, C.; Berger, S.; Caud, N.; Chen, Y.; Goldfarb, L.; Gomis, M.; et al. (Eds.) *Climate Change 2021: The Physical Science Basis. Contribution of Working Group I to the Sixth Assessment Report of the Intergovernmental Panel on Climate Change*; Cambridge University Press: Cambridge, UK; New York, NY, USA, 2023. [[CrossRef](#)]
22. Koshlyakov, M.; Panteleev, G.; Sazhina, T.G.; Yaremchuk, M. Structure and variability of the current field in the thermocline according to “Megapolygon-87” data. In *The Experiment “Megapolygon”*; Nauka: Moscow, Russia, 1992; pp. 242–250. (In Russian)
23. Gulev, S.; Ivanov, Y.; Kolinko, A.; Lappo, S.; Morozov, E. The experiment “Atlantex-90”. *Russ. Meteorol. Hydrol.* **1992**, *5*, 51–61. (In Russian)
24. Gusev, A.; Diansky, N. Numerical simulation of the world ocean circulation and its climatic variability for 1948–2007 using the INMOM. *Izv. Atmos. Ocean. Phys.* **2014**, *50*, 1–12. [[CrossRef](#)]
25. Zalesny, V.; Marchuk, G.; Agoshkov, V.; Bagno, A.; Gusev, A.; Diansky, N.; Moshonkin, S.; Tamsalu, R.; Volodin, E. Numerical simulation of large-scale ocean circulation based on the multicomponent splitting method. *Russ. J. Num. Anal. Math. Model.* **2010**, *25*, 581–609. [[CrossRef](#)]
26. Moshonkin, S.; Zalesny, V.; Gusev, A. Simulation of the Arctic–North Atlantic Ocean circulation with a two-equation k-omega turbulence parameterization. *J. Mar. Sci. Eng.* **2018**, *6*, 95. [[CrossRef](#)]
27. Byshev, V.; Figurkin, A.; Anisimov, I. Interdecadal variability in thermal structure of water in the upper active layer in the northwestern Pacific Ocean. *Dokl. Earth Sci.* **2017**, *477*, 1343–1347. [[CrossRef](#)]
28. Byshev, V.; Neiman, V.; Romanov, Y.; Serykh, I. Global atmospheric oscillations in dynamic of the recent climate. *Curr. Probl. Remote Sens. Earth Space* **2014**, *11*, 62–71. (In Russian)
29. Cheng, L.; Abraham, J.; Trenberth, K.; Fasullo, J.; Boyer, T.; Mann, M.; Zhu, J.; Wang, F.; Locarnini, R.; Li, Y.; et al. Another Year of Record Heat for the Oceans. *Adv. Atm. Sci.* **2023**, *40*, 963–974. [[CrossRef](#)] [[PubMed](#)]
30. Ivanov, Y.; Koshlyakov, M.; Monin, A. The hydrophysical Experiment “Megapolygon”. In *The Experiment “Megapolygon”*; Nauka: Moscow, Russia, 1992; pp. 3–11. (In Russian)
31. Byshev, V. On interconnection between currents and temperature in the zone of subarctic front of the Pacific Ocean (measured in the scope of “Megapolygon-87”). In *The Experiment “Megapolygon”*; Nauka: Moscow, Russia, 1992; pp. 272–290. (In Russian)
32. Byshev, V. *Synoptical and Large-Scale Variability of Ocean and the Atmosphere*; Nauka: Moscow, Russia, 2003; 343p.

33. Koshlyakov, M.; Maksimenko, N.; Panteleev, G.; Sazhina, T.G.; Yaremchuk, M. Structure and variability of the current field in the depths of the ocean according to direct measurements of currents at the “Megapolygon”. In *The Experiment “Megapolygon”*; Nauka: Moscow, Russia, 1992; pp. 251–259. (In Russian)
34. Byshev, V.; Snopkov, V. On the formation of the sea surface temperature in the energy active zone of the northwestern part of the Pacific Ocean by the example of the test site “MEGAPOLYGON”. *Russ. Meteorol. Hydrol.* **1990**, *11*, 70–77.
35. Ivanov, Y.; Morozov, E. Water transport in the Gulf Stream delta. *Dokl. Earth Sci.* **1991**, *319*, 487–490. (In Russian)
36. Bubnov, V.; Byshev, V.; Volostnykh, B.; Golenko, N.; Egorikhin, V.; Zubin, A.; Paka, V. Frontal intrathermocline lens. *Dokl. Earth Sci.* **1991**, *317*, 453–458. (In Russian)
37. Orlov, V. Approbation of a differential-parametric model of the ocean upper layer. *Oceanol. Res.* **1990**, *43*, 83–91. (In Russian)
38. Byshev, V.; Orlov, V. On the nature of the intrathermocline lens on the subpolar front in the North Atlantic. *J. Oceanol.* **1993**, *33*, 340–346. (In Russian)
39. Ivanov, Y.; Byshev, V.; Romanov, Y.; Sidorova, A. On the structure of the North Atlantic current in May–June 1990. *J. Oceanol. Res.* **2019**, *47*, 33–63. [[CrossRef](#)]
40. Baranov, E. *Structure and Dynamics of the Gulf Stream System Waters*; Hydrometeoizdat: Moscow, Russia, 1988; 252p. (In Russian)
41. Byshev, V.; Snopkov, V. Comparison of sea surface temperature (SST) at the MEGAPOLYGON based on hydrological survey data and Japanese maps and analysis of SST variability. In *The Experiment “Megapolygon”*; Nauka: Moscow, Russia, 1992; pp. 151–159. (In Russian)
42. Byshev, V.; Koprova, L.; Romanov, Y. Formation of ocean surface temperature anomalies in the Newfoundland energy active zone in May–June 1990. *Russ. Meteorol. Hydrol.* **1996**, *1*, 57–65.
43. Byshev, V.; Egorikhin, V.; Maksimenko, N.; Sobol, V. Structure and synoptical variability of the North Atlantic Current on the meridional section along 36° W in summer 1990. *Dokl. Earth Sci.* **1997**, *355*, 397–400. (In Russian)
44. Byshev, V.; Usychenko, I. Temperature structure of Gulf Stream delta waters in May and June 1990. *Dokl. Earth Sci.* **1996**, *345 A*, 133–136.
45. Byshev, V.; Koprova, L.; Navrotskaya, S.; Pozdnyakova, T.; Romanov, Y. Anomalous state of the Newfoundland energy active zone in 1990. *Dokl. Earth Sci.* **1993**, *331*, 735–738. (In Russian)
46. De Verdière, A.; Merchier, H.; Arhan, M. Mesoscale Variability Transition from the Western to the Eastern Atlantic along 48° N. *J. Phys. Oceanogr.* **1989**, *19*, 1149–1170. [[CrossRef](#)]
47. Katz, E. Diffusion of the core of Mediterranean Water above the Mid-Atlantic Ridge crest. *Deep Sea Res. Oceanogr. Abstr.* **1970**, *17*, 611–625. [[CrossRef](#)]
48. Dzerdzeyevskii, B. *Circulation Mechanisms in the Atmosphere of the Northern Hemisphere in 20th Century*; Institute of Geography: Moscow, Soviet Union, 1968; 240p. (In Russian)
49. Calendar of successive changes of the elementary circulation mechanisms over an 87-year period (1899–1985). In *Proceedings of the Meteorological Researches*; Interdepartmental Geophysical Committee of the AS of the Soviet Union: Moscow, Soviet Union, 1987; Chapter 13, pp. 29–116. (In Russian)
50. Kononova, N. *Classification of Circulation Mechanisms of the Northern Hemisphere According to L.B. Dzerdzeevskii*; Voentekhnizdat: Moscow, Russia, 2009; 371p. (In Russian)
51. Palmén, E.; Newton, C. (Eds.) *Atmospheric Circulation Systems. Their Structure and Physical Interpretation*; International Geophysics; Academic Press: New York, NY, USA, 1969; 603p.

Disclaimer/Publisher’s Note: The statements, opinions and data contained in all publications are solely those of the individual author(s) and contributor(s) and not of MDPI and/or the editor(s). MDPI and/or the editor(s) disclaim responsibility for any injury to people or property resulting from any ideas, methods, instructions or products referred to in the content.